Again `why layered, square-planar, mixed-valent cuprates alone?' - further pursuit of the `chemical' negative-***U*** route to the HTSC mechanism

2000 J. Phys.: Condens. Matter 12 R517

(http://iopscience.iop.org/0953-8984/12/43/201)

J. Phys.: Condens. Matter **12** (2000) R517–R547. Printed in the UK PII: S0953-8984(00)13003-6

REVIEW ARTICLE

Again 'why layered, square-planar, mixed-valent cuprates alone?'—further pursuit of the 'chemical' negative-U route to the HTSC mechanism

John A Wilson

H H Wills Physics Laboratory, University of Bristol, Tyndall Avenue, Bristol BS8 1TL, UK

E-mail: john.a.wilson@phys.bris.ac.uk

Received 3 April 2000

Abstract. This paper is a consolidated presentation of why the author believes the most promising way forward as regards the mechanism for high-temperature superconductivity remains with the 'chemical negative-U' interpretation, first sketched out in 1987. Many other mechanisms have been proposed over the years but none address head on the problem as to why the phenomenon is so tightly confined to the current small subset of mixed-valent cuprates. T_c in Hg-1223 under pressure is more than 450% greater than from *any* other class of superconductor. By concentrating on the materials side, and how this controls evolution in real space and k-space properties, a more tailored outlook can be gained. This includes understanding how cuprates find themselves in a unique position with regard to chemical bonding, to the delocalization of charge and to the decay of magnetism. It entails appreciation of the fine-tuning of metallization which is achieved by the choice of counter-ions, and the part which the latter play in stabilizing cuprate valencies and crystal structures. By emphasizing the fundamental role of the periodic table in this physics I wish to see the 'chemical' side to what is involved given greater consideration. It is clear whether in dealing with the HTSC materials by transport measurements or nmr or optical properties or ARPES or neutron scattering that they are 'marginal metals'. A formal Fermi liquid approach has to be pushed to the limit—and beyond. It is a pity that more high-level cluster calculations, drawing on quantum chemistry, have not been employed to attack the problem. Nowhere is that effort more greatly missed than in the need to corroborate formally the shell-closure negative-U understanding of HTSC adhered to throughout the course of the present work. I have made double-loading shell-closure fluctuations, with their termination of pdσ/σ^* bonding/antibonding interaction, and the concomitant collapse in the elevated position of the crucial $d_{x^2-y^2}$ state, the lynch pin to all HTSC events. As the paper describes, the layered square-planar crystal structure adds its own essential contribution toward the configuring of a highly restrictive set of conditions. I have attempted to incorporate a broad enough sweep of experimental results to demonstrate just how restrictive those conditions are. These any satisfactory interpretation of HTSC has necessarily and readily to embrace.

0. Introduction

Section 1 provides some general background to the HTSC materials and to the terminology to be used. Included are the questions of 'holes' in doped Mott insulators, of disorder and of inhomogeneity. Addressed too are the matters of valency and of state labelling in the given tight-binding circumstance, as also are the bond length effects issuing from changes in site charge loading. A two-subsystem environment is defined and the roles there of low site spin, the Jahn–Teller effect and RVB formation are outlined. Some discussion of stripe formation, the double-loading fluctuation and the effect of counter-ion choice conclude this section.

Section 2 sets out the mixed boson–fermion negative-U HTSC scenario for the cuprates developed in [1]. The significance of the Van Hove scattering sinks and the changes in carrier scattering through T_c are examined. Addressed too is whether the carrier pairing is 2e or 2h in nature, as is also the evident asymmetry between the effects of p-type and n-type doping. We look additionally at whether the stripe phase formation is $1q$ or $2q$ in form, and whether such structured charge segregation is of crucial importance to HTSC. The relation of the negative-U electronic mechanism to disproportionation is introduced. Laser pump–probe experiments are determined to support a measure of U^* and U_{eff} as being large and negative.

Section 3 discusses the distribution and nature of the $d_{x^2-y^2}$ states within k-space and the effect of the saddle points, and highlights the relation between these and the primary Cu–O bonding. The intermediary boson of negative-U shell-closure form in the first instance acquires the wave-vector 'π, π' $\equiv (\frac{1}{2}, \frac{1}{2})2\pi/a$, which has encouraged much confusion with antiferromagnetic spin fluctuations. The anisotropies of the situation above and below T_c, along with the pairing range, are discussed in relation to the symmetry of the superconducting order parameter.

Section 4 presents, against the 12-point analysis for HTSC materials introduced by Wilson (1987, 1988) [1], something of how the situation has filled out over the intervening years. Included are matters relating to low dimensionality, layering number, weak localization, loss of magnetism, Fermi surface nesting, the effects of Pr and Zn substitution, the inequivalence of d^1 to d^9 and finally the topic of disproportionation. This property set collectively marks out cuprate behaviour as something special within the periodic table. A key factor is the genesis of the last topic and precisely how this stands distinct from negative-U HTSC pair formation.

Section 5 examines some results from two very sensitive probes of the HTSC circumstance, neutron scattering and NQR. The results from the first study are used to make better distinction between magnetic/RVB pseudogapping and superconductive pair gapping. The results from the second are crucial to appreciating the two-subsystem nature of these systems, vital to the present negative-U interpretation of the HTSC phenomenon.

Section 6 returns to look at some details concerning the mechanism and ties in the ARPES results. Finally it draws attention to some recent theoretical works with the aim of redirecting their conclusions towards the chemical negative-U interpretation advanced here.

1. Background and terminology revisited

It is my long-standing belief [1] that theoretical treatments of the cuprate HTSC problem, and in particular (for the purposes of this paper) of negative-U treatments, are repeatedly failing to provide a proper description of the observed phenomena because they fail to register the heterogeneous mixed-valent nature of these materials. This inhomogeneity is transferred to the crucial CuO_2 planes from the substituent/dopant ions (taken initially as electron deficient) that are required to introduce metallic carrier transport here. In the absence of such doping the parent divalent 'd^9' cuprates are all Mott insulators. Even with the doping the Fermi liquid behaviour attained is of a 'marginal' form, showing a deep correlation driven and disorder supported pseudogap. This brings to the carriers at E_F not only a p-type character ($(d\sigma/dE)_{E_F}$ negative) but also a carrier number which has to be reckoned (as 'holes') from the half-filling (d^9) point of the key, E_F-bearing, $pd(e_g)\sigma^*$ band. The latter band by virtue of the Jahn–Teller distortion in these layered systems is of $d_{x^2-y^2}$ symmetry as opposed to d_{z^2}. Right through to the termination point for the superconductivity accessed with the valence modification process, the hole count p in the majority of HTSC materials is fairly closely conveyed by the dopant concentration. This particularly is the case with cation substitution (as in $(La^{3+}_{2-x}Ba^{2+}_x)CuO_4$,

where $p = x$), and usually is so under anion substitution (in say $Sr_2CuO_2^{2-}F_{2+\delta}^{1-}$, where $p = x$), and indeed often is so even if employing an 'intercalated' excess oxygen content (as in $HgBa_2CuO_{4+\delta}$, where $p = 2\delta$—when at the full mercury complement). Direct record of the inhomogeneity intrinsic to these systems first was gained in nqr work [2], and has since been secured through other local probes of the structural and electronic environment such as EXAFS, PDF and Mossbauer (see Wilson 1998 [1]). Essentially two site types are present and their spatial distribution defines the two-subsystem structure. The 'sites' will nominally be termed 'divalent' and 'trivalent'.

In the cuprates, unlike say the corresponding manganates, we are not in the hard ionic limit, and one has to appreciate that we are with the above words labelling not just the copper atoms alone but the entire coordination units directly proximate (or not so) to a substitutent species. Standard band structure calculations undertaken for the parent divalent cuprates show that because the relative energy locations of the atomic $d_{x^2-y^2}$ state of the coppers and the $p_{x,y}$ states of the coordinating oxygens are very close, they generate an x^2–y^2 symmetry conduction band which is fairly wide (although overstated in simple LDA at more than 2 eV). Real space charge plots [3] correspondingly reflect the heavy state mixing involved in this $pd(e_g)\sigma^*$ antibonding hybrid band. Electron wavefunctions near E_F are evaluated as running approximately 50:50 over the copper and the oxygen sublattices. Hence the sorts of electron configuration that one can expect for the crucial CuO_2 basal planar units in a 'divalent' or a 'trivalent' situation might well find representation respectively as $p^{5.8}p^{5.8}d^{9.4}$ and $p^{5.6}p^{5.6}d^{8.8}$. It is seen here that the former set is one electron short of total shell closure at $p^6p^6d^{10}$, while the latter set is short by two electrons; hence the overall electron counting terminology 'divalent' and 'trivalent' for these sites *vis-à-vis* 'monovalent' Cu_2O and its full-shell p^6d^{10} complement. Throughout my earlier work the above states (and the subsystems which they build) have been labelled $^9Cu_{II}^0$ and $^8Cu_{III}^0$, expanding upon standard chemical notation. This permits further extension then to $^9Cu_{III}^{1-}$ and $^{10}Cu_{III}^{2-}$ to describe respectively (i) the single electron fluctuation that brings metallicity to the mixed-valent system, and (ii) the double or negative-U fluctuation which is perceived by the author to be responsible for HTSC in these systems within the modelling developed at length in [1].

A static change in the formal electron count within a coordination unit is inevitably associated with a change there in the M–X bond length. This is very marked whenever, as for the cuprates, $\sigma^{(*)}$ states are involved: observe how the TM–X distance steadily lengthens from La_2NiO_4 to La_2CuO_4 to La_2ZnO_4 as the antibonding electron complement is built up through the sequence d^8–d^9–d^{10}. In the layered mixed-valent cuprates themselves a structural response is incurred in two ways: (i) by a formal increase in the local Madelung potential on going from Cu_{II} to Cu_{III} and (ii) by the occurrence of a severe Jahn–Teller distortion at Cu_{II} sites, absent for Cu_{III} (Wilson 1998) [1]. In the HTSC cuprates the two effects act to oppose each other within the basal plane, but they reinforce in the c-axis direction. EXAFS data are able to provide a clear record of the strong c-axis accommodation occurring locally within the two-subsystem environment ([4]; Wilson 1998 [1]). c-axis pressure is as a result observed to have a notably strong effect upon HTSC materials, decreasing T_c for all p, this from the diminished differentiation between the two subsystems. For under and optimally doped material [5] in-plane compressional stress consistently produces the inverse effect.

Our early work treated the two-subsystem network as being of totally random form, given the random distribution of substituent atoms known to be attained in the customary high-temperature synthesis of HTSC cuprates. That view was expressed in figure 4 of Wilson (1988) [1], where it was noted that the favoured dopant concentration for HTSC of $p \sim 0.16$ marks the point at which free percolation first would be possible over the Cu_{III} driven subsystem. It is also roughly where 50% of the coordination units have become affected by the doping,

with maximization of the interface between the two subsystems in regard to charge transfer. The levels of hybridization and structural disruption have moreover by then become sufficient to suppress standard SRO antiferromagnetic ordering fully in favour of resonant valence bond (RVB) behaviour [6, 7]. Recall that for the HTSC cuprates we find an $S = \frac{1}{2}$ condition on the Cu_{II} centres, while the Cu_{III} centres acquire the $S = 0$ low-spin configuration observed in $NaCuO_2$, $LaCuO_3$ etc. Quite generally $S = \frac{1}{2}$ sites in a delocalizing environment such as the present one do not possess long-term local spin alignment stability comparable to that obtained for a multi-electron configuration (e.g. in d^2 $S = 1$ CrO_2); this appears due to lack of net spin under the relevant site charge fluctuations—currently to $^{10}Cu^{1-}_{II}$ and $^{8}Cu^{1+}_{II}$ from $^{9}Cu^{0}_{II}$.

From neutron scattering it steadily became evident that the actual organization of dopant-introduced charge in the cuprates does not remain strictly anchored about the dopant centres (taken here as randomly dispersed). The dopant-introduced holes become driven by a mixture of Coulomb forces and lattice constraints to adjust somewhat towards a rectilinear/crossed microdistribution. Neutron scattering is particularly sensitive to the spin ordering which in the wake of charge redeployment starts to develop within the hole-vacated Cu_{II} subsystem, as the latter converts towards a more regularized RVB square-plaquet structure (Wilson 1998, Wilson and Zahrir 1997) [1]. If this organization proceeds too far, as in LBCO near $x = \frac{1}{8}$, superconductivity can become strongly impaired by the re-emergence of some form of antiferromagnetic order at low temperatures. This is rare, though, and already is much less strongly in evidence in the more metallic LSCO system. Here T_c minimizes only weakly at $x = 0.115$, rather than strongly at $\frac{1}{8}$. With the LSCO case it is observed, however, that the disordering, charge-localizing effect of the isovalent substitution of some La^{3+} by Nd^{3+} reintroduces and indeed augments the situation met within the Nd-free Ba system. The above emergent 'stripe phase' organization first was picked up by neutron diffraction, initially with the incommensurate spotting recorded in inelastic scattering from LSCO [8], and then with the elastic counterpart first from $(La/Nd/Sr)_2CuO_4$ and finally LSCO itself around $x = 0.12$ [9].

I remarked back in 1994 (Wilson 1994a) [1] that given such manifestly inhomogeneous systems one ought not to be looking toward a simple uniform superconducting order parameter, particularly when the (basal) superconducting coherence length is only $\sim 4\,a_0$. Indeed the pair radius itself is likely to be little larger than a unit cell or so (i.e. ~ 5 Å). c-axis coherence lengths are known to be less even than this, making c-axis tunnelling phenomena open to strong distinction from basal plane behaviour [10].

The general inhomogeneity and the very significant anisotropy in the c-axis versus basal plane metallicity—as too in the superconductive coupling—open up the way to a highly local negative-U scenario for HTSC (Wilson 1987, 1988, 1989) [1]. Recall here that the spin-paired state becomes protected as far as possible from the pair-breaking processes ordinarily prevalent in magnetic systems close to the Mott transition as a result of the indicated RVB singlet formation. RVB behaviour is specific to the $S = \frac{1}{2}$ circumstance [6] (here of $^{9}Cu^{0}_{II}$). As I have argued repeatedly, however, the essential factor in the appearance of HTSC, and in practice one unique to the mixed-valent cuprates, is the closed-shell energetics being accessed with the double-loading fluctuation $^{10}Cu^{2-}_{III}$. It is because of this special circumstance within what is afforded by the periodic table that in the original publications of 1987 and 1988 [1] I chose to term this particular negative-U route to HTSC 'chemical'.

At present there is a vogue for strongly advocating the role of stripe formation in driving the very appearance of HTSC [11, 12]. Personally I would cast charge stripe organization in a somewhat less central role. The prime factor is the existence of the two-subsystem environment rather than of some set geometric form. Emery and Kivelson [11] wish to introduce with the stripes notions of quantum fluctuation and constraints upon quasiparticle kinetic energy as sourcing carrier pairing. Bianconi *et al* [12] on the other hand see the ensuing modifications

in band structural form as driving the pairing. While there are indications that charge stripe tendencies are in fact current in all the HTSC cuprates (and we ourselves have recently written about this with regard to Hg-1201 and BSCCO-2212 (Farbod *et al* 2000 [1])), it is apparent that such organization becomes weaker, not stronger, upon moving to systems of higher T_c^{max} than LSCO. As was argued by Wilson (1994a) [1], the role of counter-ion choice in governing the progression of HTSC onset temperatures is very sensitive: too ionic, as with La/Ba, and the system becomes too magnetic: too covalent and delocalized, as for Bi/Sr, and T_c falls back again. Hg/Ba looks to provide the optimal electronic environment.

2. Incorporating some key new results on the magnitude of U_{eff}, on the signs of the normal carriers and pairs, and on the pair lifetime

Many others pursuing a view of HTSC supported by a negative-U scenario, such as Alexandrov *et al* [13] or Trivedi and Randeria [14], would seem, as was indicated at the outset of this paper, to be blocked in their progress because the models they employ invariably are treated as homogeneous. The problem then is that all the quasiparticles become able to pair too freely. The events at T_c become those of a Bose–Einstein condensation of pre-existing bosons, this occurring at the point where phase coherence becomes established across the pre-paired system. However many measurements, such as specific heat [15], would not support such a viewpoint, and indeed indicate a concentration of pairs even below T_c that is surprisingly diminished. The famous Uemura plot [16], derived from μSR data through its relation to the penetration depth λ and so to the superfluid pair density n_s, indeed would indicate that T_c actually is of the order of one-fifth that expected of a simple homogeneous B–E condensation. What is more the broad range of the Uemura plot associates the superconducting behaviour of the HTSC cuprates with that of various other non-standard superconducting families such as the alkali metal fullerides, (Ba/K)BiO_3, and the Chevrel cluster phases, right on down to the organic and heavy-fermion superconductors. The fermionic or rather mixed aspects to what is afoot surely are made evident here. This dual character has been surprisingly little investigated formally beyond the work of Micnas *et al* [17] and Friedberg and Lee [18]. Even there not much is ventured concerning the possible microscopics of the pairing interaction, nor of what defines the two-subsystem behaviour, nor what is the cause of the strong pair-breaking. It is my own view that what is responsible in the cuprates for the depressed and ineffectual pair count below T_c is of like origin to the chronic scattering evident for the quasiparticles above T_c, namely a combination of the mixed-valent microstructure, the near-magnetic environment and the amplified Van Hove singularity scattering sink states around $\{\frac{1}{2}, 0\}2\pi/a$ (Wilson 1996) [1]. Above T_c the charge and spin pseudogapping and the resulting positive sign impressed on the carriers within a simple band significantly less than half full (virtually independent of structural detail) has in large measure to be ascribed to general correlation and disorder rather than specifically to widespread pre-pairing. Pseudo-gapping is evident in very many correlated and/or mixed TM systems which ultimately display CDWs, SDWs or whatever. Particularly noteworthy for the systems grouped together by the Uemura plot is that each exhibits very marked electron scattering in the normal state, for which the resistivity takes a power law form $\rho \propto T^n (n < 2)$, often to quite high temperature. In the HTSC materials such electron scattering indeed is observed to hold up to such high T and ρ values that it clearly has passed over from what may be incorporated within a normal quasiparticle band framework into individual classical particle collisions.

It is evident that upon passage below T_c the effects of this chronic electronic scattering are very considerably lessened, as the dynamic screening becomes much increased. The rapid fall-away in electronic thermal resistivity deduced from measurements of the thermal conductance, together with the sharp decline in nmr of the spin–lattice and spin–spin relaxation rates, have

long been seen to characterize this. While the above would indicate that the superconducting state has to some degree become less anomalous than the normal state, photo-emission from the superconducting state clearly reveals it to remain anomalous. Whatever happens right at E_F, the great body of CB electron states certainly do not suddenly become 'standardized' once below T_c [19]. The effects of the evolving pseudogapping remain evident in the IR reflectivity below T_c, especially for c-axis polarization [20]. The Raman results likewise remain abnormal [21], even after allowing for the fact that we are dealing here with a non-s-wave symmetry superconductor. While in standard optical work the superconducting gap is not itself much in evidence, there do show up close to T_c sharp Raman phonon line-shift and line-width changes which disclose the significant self-energy changes arising there [22].

From what has been said it is surprising that so much theoretical probing has been carried forward in a mean-field framework, closely tied to the BCS and Bogoliubov–de Gennes formalisms of traditional superconductivity. It must be recalled that all present evidence is that the condensate pair count is significantly below the number of electrons in the $d_{x^2-y^2}$ band divided by two, as would be obtained within a mean-field account of standard superconductivity.

Perhaps it might be felt that the observed lower pair count has to refer to a condensation of the 'hole' carriers of the normal state cuprates, their numbers reckoned from half filling. Surprisingly the great majority of workers indeed do cast their theories in terms of a pairing of holes, including those who concentrate on negative-U routes to HTSC, such as the previously mentioned schools of thought represented by Micnas *et al* [17], Alexandrov *et al* [13], Randeria, Trivedi *et al* [14] and Emery and Kivelson [11]. Experiment would suggest however that this construction on events presents an unnecessary and indeed unwarranted barrier to identification of the actual origin of the negative-U coupling advocated. It was noted by Dunne and Spiller [23] as early as 1992 that the sign of the outcome of London moment experiments performed on YBCO etc [24] would indicate that the carrier pairing responsible is, as is customary, essentially of electrons as distinct from holes. That conclusion finds support in the reversal of sign from positive to negative observed in the transverse Hall conductance in the vortex-free fluctuation range just *above* T_c—in addition to below T_c [25]. This would accord with my own view of what is occurring, where pairing rests upon the localized filling by electrons of the x^2-y^2 state in a two-electron intersubsystem fluctuation, this falling in near-resonance with E_F, and to be represented by

$$^{9}\mathrm{Cu}^{0}_{II} + {}^{9}\mathrm{Cu}^{0}_{II} + {}^{8}\mathrm{Cu}^{0}_{III} \longrightarrow {}^{8}\mathrm{Cu}^{+}_{II} + {}^{8}\mathrm{Cu}^{+}_{II} + {}^{10}\mathrm{Cu}^{2-}_{III}.$$

The $^{8}\mathrm{Cu}^{0}_{III}$ sites drawing in electrons in this manner are most likely to reside within the positive charge stripes. Remember in the stripes only a subset of the 'sites' there are going actually to 'coincide' with the substituent dopant atoms, the latter being randomly distributed within current samples. Accordingly the number of CuO_2 units 'primed' to perform the above electron pairing process becomes rather small—only those experiencing the deeper Madelung potential. The stripes are likely to be pinned to such cells, and indeed these may then come to define x, y crossing points within the array.

It would seem that not enough work has been undertaken on the 'stripe' diffraction peak intensities to assert definitively whether or not we have a uniaxially striped $1q$ array rather than a $2q$ crossed array as selected in my own presentation of 1997 and 1998 [1]. The latter choice was made following my experience with CDW arrays. Both crossed and uniaxial phases are observed in 1T-TaS_2 and $NbTe_2$, but multi-$\boldsymbol{q}$ arrays are more usual in low-amplitude systems like the present [26]. Fluctuations in the adopted geometry automatically will become less strongly defined as an incommensurate system moves away from higher-order commensurability and the charged discommensurations introduced via the commensurability routine become more tightly packed. Those wishing to pictorialize the effects in stripe phase behaviour, or alterna-

tively in field vortex structures, would do well to study the CDW discommensuration pictures we generated by electron microscopy from 2H-TaS_2 etc [27]. It may be recalled that the success we encountered in dark-field imaging those arrays rested not upon line but upon areal contrast. This arose in consequence there of the orthorhombic symmetry breaking imposed upon the 2H structure by the mutual stacking and phasing of the two MX_2 sandwiches per unit cell.

Besides the question as to whether in the II/III mixed-valent cuprates we are dealing with electron or with hole pairing, it is necessary for any potential theory of HTSC to address additionally the patent asymmetry between decreasing the overall electron count within the $d_{x^2-y^2}$ band below d^9 (as in $(La/Sr)_2CuO_4$) versus nominally increasing it above d^9 (as in $(Nd/Ce)_2CuO_4$ [28] and $(Nd/Sr)CuO_2$ [29]). T_c values reported for the latter 'electron-doped' systems always in fact are much lower than for the 'hole-doped' systems, though still abnormally high—in the above examples 20 and 40 K respectively. My own interpretation of events would have some difficulty in coping even with such data, were the systems indeed to be correctly represented by the above formulae. However it is widely recognized when working with these 'n-type' materials that it is not straightforward to prepare the superconductive samples. The precise oxidation and thermal treatment details are critical and clearly involve the setting up of a complex microstructure. Several times it has been expressed that in reality these systems still lie to the low side of the d^9 count [28]. This is able to come about when the effective *local* oxygen content stands in excess of integer stoichiometry, an accepted way to secure superconductivity in $La_2CuO_{4+\delta}$, $HgBa_2CuO_{4+\delta}$ etc. In oxygen-inserted systems the microstructural detail frequently emerges as being far more complex than most theorists are pleased to contemplate. We demonstrated by electron microscopy ten years ago for $La_2CuO_{4+\delta}$ that the latter achieves a certain parity of behaviour with $(La_{1.85}Sr_{0.15})CuO_4$ at surprisingly low δ values by virtue of a 'microscopic' spinodal segregation of the excess oxygen content (Ryder *et al* 1991) [1]. More recently (Farbod *et al* 2000, Wilson and Farbod 2000) [1] we have drawn attention through Seebeck work to the complex behaviour in mercury-deficient $HgBa_2CuO_{4+\delta}$. This lies outside the customary $T_c(p)$ prescription of Presland *et al* [30], displaying a marked deviation from the widely applicable relation $p = 2\delta$. Recent work on the (Nd/Ce)-type superconducting materials affirms strongly that they (and n-doped PSYCO also) indeed still fall effectively to the *low* count side of the d^9 divide [31], thereby emphatically reinforcing the asymmetry outstanding between the II/III and II/I mixed-valent cuprate materials.

One of the recurrent and somewhat disturbing features throughout the progress of HTSC has been the apparent ease with which *a posteriori* so much numerical modelling can be made to accommodate the (selected) facts just 'perfectly', whatever the form of microscopics favoured. These have included van Hove singularities, Fermi surface nesting, spin fluctuations, Jahn–Teller effects, polarons, negative-U, etc. Essentially this reflects the small energy scale within which superconductivity operates. A slight (in)judicious bending of one or two numerical parameters is able radically to transform the outcome. It was this type of problem when dealing with the phasing of discommensurate CDWs relative to each other (in a multi-axis geometry) and then onto the lattice itself [32] that provided a warning to the author of just how difficult it is at this level to separate charge, spin and lattice contributions to the internal energy and entropy of a system.

CDWs and other incommensurate and discommensurate conditions are of course very much more widespread than was realized 30 years ago. One might regard them as a peripheral if interesting sideshow to the behaviour of their hosts such as α-U, NaV_2O_5, SiO_2, PbO, $HfTe_5$, etc: a ubiquitous low-energy symmetry breaking settlement into the detailed ground state. However it is evident from all sides that the HTSC behaviour of the II/III mixed-valent cuprates is not to be presented in quite this manner, for it is unique, it is lacking in detailed structural and electronic variability and it is remarkably robust towards impurities, including

magnetic ones. As such HTSC is unlikely then to be low energy in origin, even if relatively low energy in its final *effective* pair binding stability.

To consider an electronic (as distinct from lattice polaronic) route to negative-U superconductivity admits two factors favourable to the empirical record: (i) it is able to engage much higher energies and (ii) it is likely to be much less frequently feasible. In a TM circumstance such as the cuprate one, positioned so close to the Mott transition, state double loading is an event that inevitably must entail very significant Coulombic on-site repulsion energies ∼3–4 eV. In order to negate this—and more—we are looking therefore towards implicated energies well beyond spin energies in the narrow magnetic sense. We are addressing chemical bonding energies, correlation energies that are not normally made explicit within the customary band structural approach to solid state work. Regrettably physicists have paid remarkably little attention to the question for example of valence disproportionation (as in 's^1' TlS or 'd^7' PtI_3), or even to valence differentiation (as in $TlInS_2$ or $CuFeS_2$).

I have endeavoured to highlight such matters in a couple of recent papers (Wilson 1999, 2000) [1]. The first of these relates to femto-second laser pump–probe data from the HTSC materials, supported by the results of thermo-modulation NIR spectroscopy. There the anomalous energies demonstrated as making meaningful contact with the HTSC phenomenon lie in the range of 1.5–2 eV per *electron*. In figure 1 taken from Wilson (1998) [1], J' represents

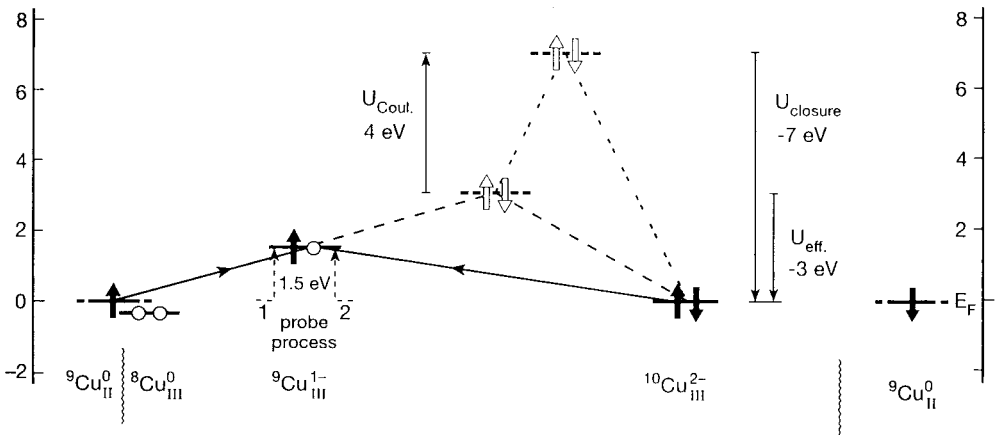

Figure 1. Resonant negative-U model from Wilson (1987, 1988) [1], where the state symbols used are introduced. The latter indicate a local coordination unit's nominal cation valence along with its instantaneous charge loading, both current and as a deviation from the norm. The figure indicates the fluctuational state-loading energies for the trivalent ('doped') site loading sequence $^8Cu^0_{III}$, $^9Cu^{1-}_{III}$, $^{10}Cu^{2-}_{III}$ to be a re-entrant one. This is due to p^6d^{10} shell closure and the accompanying collapse in σ/σ^* p/d interactions. Because of some permanent, metallizing, charge transfer between the two subsystems of the mixed-valent situation, ground states $^9Cu^0_{II0}$ and $^8Cu^0_{III}$ are effectively brought to a common Fermi energy. In optimally doped HTSC systems the negative-U double-loading fluctuational state $^{10}Cu^{2-}_{III}$ becomes positioned in near-resonance with E_F. This makes U_{eff} (per electron) −1.5 eV, in line with the value extracted from the femtosecond laser pump–probe experiments (Wilson 2000) [1]. Note that the customary definition

$$U = [(E_{n+2} - E_{n+1}) - (E_{n+1} - E_n)] = (E_{n+2} + E_n) - 2E_{n+1}$$

becomes in the present case

$$U = E(d^{10}) + E(d^8) - 2E(d^9)$$

where

$$U = U_{eff} = U_{coul} - U_{shell\ closure}.$$

With U_{coul} = +3 eV and $U_{shell\ closure}$ = −6 eV we reach U_{eff} = −3 eV per pair or −1.5 eV per electron, as the experiments would endorse. (NB: in text $U_{shell\ closure}$ contracted to U^*.)

the intersite (i.e. inter-subsystem) charge transfer energy (labelled in pseudospin fashion). The final double-loading situation as evaluated relative to an E_F tied to the left hand state in the figure is such that

$$2J' + U_{coul} + U^* = E_b$$

the pair binding energy. The numbers we favour here, and ones which experiment would now appear to support (Wilson 2000) [1], are

$$J' = 1.5 \text{ eV} \qquad U_{coul} = 3 \text{ eV} \qquad E_b = 0 - \varepsilon \text{ eV}.$$

This makes $U^* = -6$ eV for the true negative-U physics, and thus $U_{eff} \equiv U^* - U_{coul} = -3$ eV per pair. The latter is the value of negative U needed for formal insertion into the customary Hubbard Hamiltonian. Such a negative U_{eff} value is nearly an order of magnitude greater than what lattice polaronic/bipolaronic modelling could support. Even on an electronic scale of energies the above has to issue from unusual circumstances. These I have attributed to shell-closure effects, wherein the key double-loading charge transfer fluctuation ($^{10}Cu^{2-}_{III}$) precipitates collapse of the antibonding σ^* state within the high-valent electron-receiving Cu–O coordination unit. Prior to occupation the empty σ^* band had been driven many eV above its filled bonding σ counterpart. The effects of sub-shell and full-shell closure are precisely those involved in disproportionation. For TM materials, such behaviour draws upon an added stability (in appropriate local bonding geometries) at d^2, d^4, d^6, d^8 and particularly d^{10} site electron counts (see section 4).

The second of the above recent papers (Wilson 1999) [1] dealing with these matters relates to HfNCl, or rather to HfNCl.$Li_x(THF)_y$, the new 25 K superconductor. Disproportionation is widely encountered in Hf_{III} systems. As Wilson (1999) [1] highlights, however, something distinct from disproportionation is called for to support negative-U superconductivity. The re-entrant nature of the double- versus single-electron loading energies needs to be sufficiently marked for it to confer upon the electron pairing promoted an appreciable metastability; this is especially so when one wishes to see that pair state energy set in near-resonance to E_F.

3. Questions in negative-U pair binding of orientation and range

At this point it would be advisable to review why the σ^* '$d_{x^2-y^2}$' band in the HTSC square-planar cuprates acquires the dispersional form that it does. The band is lowest at the Γ point $(0, 0)$ and highest at the corners $\{\frac{1}{2}, \frac{1}{2}\}2\pi/a$ of the Brillouin zone (X and/or Y points), while at the M points, the cell edge mid-points $\{0, \frac{1}{2}\}2\pi/a$, one is in the vicinity of a Van Hove singularity (VHs). At half-filling the energy of the latter is close to E_F. The VHs is a topological requirement of any single 2D band. In the present near-symmetric sinusoidal band it in fact comes just a little way below the band centre energy. For a 2D crystal structure this VHs takes the form of a logarithmic saddle-point divergence. In the real case weak 3D coupling rounds off that DOS divergence. For those cuprates with a multi-layered unit cell and associated multi-sheeted band structure the VHs will correspondingly be split. Photoemission to date has not resolved any such splitting—a mark of the marginal, highly correlated nature of these systems and the short quasiparticle coherent state lifetimes, particularly in the c-direction. The strong correlation has the effect of extending the Van Hove singularities [33] and a Fermi surface instability can result [34]. Photoemission reveals that the carriers which are tending to disappear from the Hall coefficient register, to appear localized in nmr work and to produce a non-monotonic change in chemical potential [35], are precisely those in the vicinity of the saddle points, where masses are high, and where charge and then spin pseudo-gapping sets in strongly below some characteristic T^* [36]. The lowest-mass carriers are those running

in the $\{k, k\}$-directions, for which $\boldsymbol{k}_F$ is somewhat less than $(\pi/2, \pi/2)1/a$. Under a d-wave symmetry gapping scenario the latter constitute the ungapped states in the superconducting as well as pseudogap conditions.

Note that in real space the light-mass $\boldsymbol{k}$-states take the direction of the O–O 45° overlap within the CuO_2 chessboard array and are governed largely by the n.n.n. overlap integral, t', in customary tight-binding Hamiltonian notation. t' in the present case is $\sim 0.3\ t$, where t, the axial Cu–O near-neighbour overlap integral, is ~ 0.25 eV. The primary Cu–O bonds are directed parallel to the k-space saddle-point directions, ΓM. The band dispersion in this axial direction is only half of that in the 45° ΓX (ΓY) directions, there being only one here of the two orthogonal directions with ψ phased in antibonding fashion. By contrast for the diagonal direction of the corner-point state both axial relative phasings are simultaneously arrayed in full antibonding fashion; i.e. it is at the X/Y points that the pdσ^* band becomes maximally separated from its bonding pdσ counterpart. Figure 2 illustrates in real space this maximally antibonding state associated with the BZ corners. States in the vicinity of the cell corners accordingly are only rarely occupied in normal circumstances as single-electron fluctuations. The figure finally portrays the Γ-point state, which is bonding neutral.

We are in a position now to discuss the transport and magnetic characteristics of the system. In the basal plane much of the current is carried by the diagonal states, although after directional integration the conductivity remains isotropic by symmetry (when taken as here to be pseudo-tetragonal). Note that bulk transport in the normal state usually is basally isotropic, despite the incipient localization of the states in the vicinity of the saddle points. In the YBCO materials however the chains now present naturally render the total response distinctly orthorhombic. This indeed shows up within optical work below T_c, both in the penetration depth λ as well as in the d.c. conductivity itself [37]. However of much greater significance is the *four*fold basal-plane anisotropy found in all HTSC materials in the upper critical field H_{c2} [38]. Since the coupled length is here ξ, the coherence length, the $d_{x^2-y^2}$ symmetry lying at the heart of the superconducting phenomenon becomes directly and simply revealed. The same basal fourfold anisotropy near T_c and below similarly is in evidence in magneto-resistance (Hussey *et al* 1996) [39], magneto-torque (Willemin *et al* 1998) [39], thermal conductivity (Aubin *et al* 1997) [40] and specific heat (Khlopkin *et al* 1997) [40] measurements. As with the tunnelling results, it is not totally resolved at this point as to whether the associated superconducting order parameter is really pure $d_{x^2-y^2}$, or has in some way or another further symmetries admixed. Some experiments would indicate one thing (e.g. ARPES [41]), some another (e.g. c-axis tunnelling [42]). As was expressed earlier (Wilson 1994a, Wilson and Zahrir 1997) [1], because the cuprate HTSC systems are often not tetragonal but orthorhombic, and since they are also two subsystem in form with mixed-valent and incipient stripe phase microstructure, it is not immediately clear why a simple order parameter ought to be operative. That will depend greatly upon the range of the pair coupling potential.

Let us now within the above framework look at what is happening from a k-space perspective in the proposed negative-U treatment of HTSC. The carriers being gapped below T_c are, for a dominantly $d_{x^2-y^2}$ superconducting geometry, those in the vicinity of the saddle points, as continues to be true also of the pseudogap condition above T_c. The non-dispersive high-mass nature of these states at all stages opens them to correlated coupling, Mott localization and disorder supported gapping. The closer to half-filling, the greater naturally becomes the impairment of the Fermi liquid behaviour around the M points. The susceptible states are many in number, and worse yet, as is illustrated in figure 3, their complementary empty ones provide an extensive scattering sink for the high-mobility carriers from the 45° directions. Such in- and out-of-sink transfers are seen as being a major source of the chronic electron scattering evident in these systems, where resistivity endlessly rises as the temperature rises

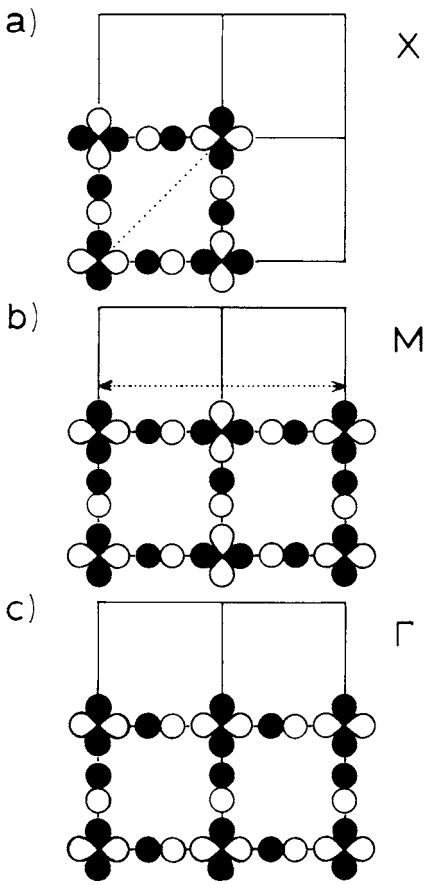

Figure 2. The phasing of the dpσ^* wavefunction in the basal square-planar CuO_2 array at (a) the zone corner X-point wavevector $(\frac{1}{2}, \frac{1}{2})2\pi/a \equiv$ 'π, π', antibonding along both Cu–O bond directions, (b) the M-point wavevector $(\frac{1}{2}, 0)2\pi/a$, antibonding along just one Cu–O bond direction and (c) the Γ-point zone centre wavevector, which overall is non-bonding. The cell corner state is maximally antibonding and empty in the cuprates, except during fluctuations $^{10}Cu^{1-}_{II}$ and $^{10}Cu^{2-}_{III}$.

and the extent of the perturbed Fermi surface regions steadily expands. Such heavy, near-localized, incoherent electrons are well matched to RVB spin coupling. Furthermore, because of their very low particle velocity (as distinct from crystal momentum), these electrons will interact together strongly in direct non-retarded fashion. As figure 3 illustrates, a heavy carrier–carrier scattering combination into a composite electronic pair state will locate that new $S = 0$ entity in k-space near the Brillouin zone corners. Such k-states are precisely those which as regards fermionic content would be maximally antibonding. Now however, given the double occupancy promoted under the negative-U interaction of local shell closure, the new bosonic k-state can drop back in *energy* so as to become effectively degenerate with E_F, the latter situation conferring a reasonably high matrix element upon the process. Being created from electrons which were virtually dispersionless, the boson state will accordingly be of very low velocity and not subject to strong scattering. The above is seen as the route by which a metastable negative-U superconductive pair population can be created. Wilson (2000) [1] interpreted the femtosecond laser pump-probe experiments as indicating a longer than 10^{-8}

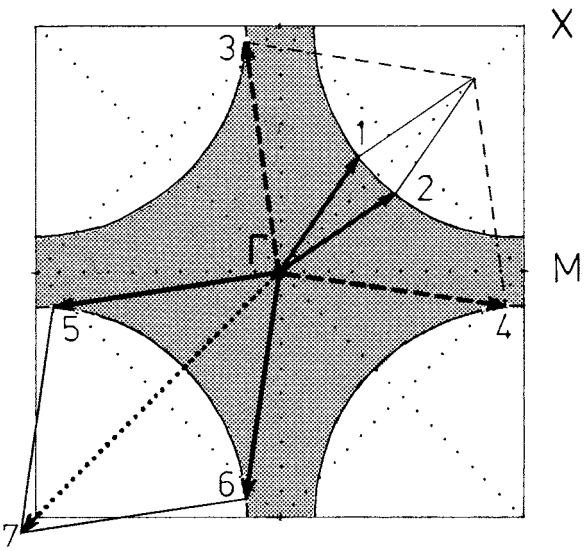

Figure 3. The Fermi surface in the pd(e_g)σ^* band and the principal scattering wavevectors. In the top right is shown the scattering of two light-mass carriers near the zone diagonal direction into the high-mass M-point saddles. In the bottom left two such low-velocity fermions in these scattering sinks combine into a pair fluctuation initially with wavevector close to the zone corner, maximally antibonding for fermions. In the relaxed form of a negative-U double-loading $^{10}Cu^{2-}_{II\,I}$ fluctuation, however, the state energy becomes near-resonant with E_F. This virtual coupling of the electrons through the negative-U fluctuation leads below T_c directly to maximal superconductive gapping of the Fermi surface states at the saddles, i.e. presents a gapping symmetry of principally d-wave form that is greatest along the Cu–O bond directions.

second timescale for the (pumped) bosonic pair lifetime.

In the above scheme one notes that formally the fermion pair coupling is mediated by the intermediary negative-U boson in a fashion not entirely unlike the BCS employment of phonons. Now however the process is fully electronic, and we have escaped from the upper limitation set on T_c by θ_D in the BCS equation $T_c = \theta_D \exp(-1/N(0)V)$. The spin fluctuation interpretation of HTSC likewise would replace $k\theta_D$ by an electronic energy, the spin exchange energy. The latter though is still not a large energy ($\sim$0.1 eV), and the general evidence is that we are not in an especially strong-coupling regime to compensate for this. It is apparent moreover that very high T_c values have to be reached in precisely those systems for which the static magnetic characteristics are fast ebbing away. For example in BSCCO-2212 at optimal doping the paramagnetic contribution to the static susceptibility is low ($\sim +250 \times 10^{-6}$ cgs units per mole Cu) and it has become virtually temperature independent [43]. In addition neutron spin scattering is now much more diffuse, with the *in*commensurate *in*elastic spotting observed around the X/Y 'π, π' points in LSCO and YBCO-123 yet to be recorded for BSCCO [44]. What however it has been possible to uncover for BSCCO-2212 below T_c using polarized (i.e. spin-flip sensitive) inelastic neutron scattering is a broad peak analogous to the sharp 'resonance peak' witnessed in $YBa_2Cu_3O_7$ at 41 meV [45]. For optimally doped BSCCO-2212 the corresponding energy is 43 meV [44]. Both values are very similar to the maximal 0 K superconducting gap energies, $2\Delta(0)$, of the antinodal ΓM direction that at optimal doping can be extracted from nmr [46], tunnelling [47] and electronic Raman spectroscopy [48], as well as photoemission [41]. The situation in BSCCO should, in fact, supply a clearer view of just what the crucial circumstances are in HTSC than can the more easily produced but less typical

LSCO and YBCO materials. The specific heat results from Junod *et al* on BSCCO-2212 in a magnetic field provide a fine example of the relative state of affairs [49]. Walstedt *et al* emphasized way back in 1991 just how weakly T_c itself actually is defined in BSCCO-2212, whether in Knight shift or in relaxation rate measurements [46].

Since those having close association with neutron scattering and nmr work often have been much engaged with magnetic problems, it is not altogether unexpected that they should resort to a magnetic interpretation of the HTSC data [50]. That inclination is of course greatly reinforced by the observation that the interesting 'spin' action in the Brillouin zone occurs around the wavevectors $\{\pi, \pi\}$. The latter are precisely the wavevectors of the antiferromagnetic ground state in these systems at the parent Mott-insulating compositions $YBa_2Cu_3O_6$, La_2CuO_4 etc. The spin fluctuation interpretation of HTSC from Millis, Pines, Monthoux and coworkers is framed around an empirical normal state q-dependent susceptibility formulated as

$$\chi(\boldsymbol{q}, \omega) = \chi_Q/[1 + (\boldsymbol{q} - \boldsymbol{Q})^2\xi^2 - \mathrm{i}\omega/\omega_{sf} - \omega^2\xi^2/c_{sw}^2] \qquad \text{(with } \chi_Q \text{ an adjustable constant)}$$

or

$$\chi''(\boldsymbol{q}, \omega) = \pi\frac{\chi_0(T)}{\Gamma_0(T)}\omega\left[\frac{1 + \beta(T)(\xi/a)^4}{1 + (\boldsymbol{q} - \boldsymbol{Q})^2\xi^2}\right] \qquad \text{where } \boldsymbol{Q} = \{\pi, \pi\}.$$

However, for this approach with its inserted strong peaking in susceptibility at $\boldsymbol{Q} = \{\pi, \pi\}$ to progress suitably, that peaking has to grow more and more pronounced in systems for which T_c^{opt} is rising, exactly at the stage where the general magnetic coupling is falling right away.

What I am advocating through the present body of work is that the operative peaking in the generalized susceptibility should not be ascribed to standard spin fluctuations, but instead to negative-U shell-closure fluctuations. The latter are equally of a spin-paired two-sublattice nature (locally completing both Cu d and O p shells), and it is easy in the circumstances to see how events may be misread as antiferromagnetism. The boson wavevector is much the same. Now however the energies behind the pairing are far greater, making the outcome more robust toward p/d hybridization and impurity effects. Above all, they are more uniquely sourced. The spin fluctuation scenario (just as with the polaronic one) should not be expected to find itself so notably confined to the cuprates as the present situation clearly is. Of all the systems demonstrating anything remotely like HTSC to have emerged over the past dozen years, only the $(Ba/K)BiO_3$ [51] and Rb_3C_{60} [52] families come anywhere near close to mimicking the cuprates. Those materials as non-TM systems are free from any significant magnetic activity. By contrast both verge upon disproportionation and two-subsystem behaviour, and indeed they possess many additional features, not least their association with the Uemura plot [16], which couple them to the cuprates and point more to electronic negative-U behaviour and away from a magnetic interpretation of events. Shell- and sub-shell-closure effects surely are being grossly neglected in all present formal theoretical treatments.

Not infrequently it is assumed with a local negative-U scenario that the superconducting order parameter must inevitably be s-wave, and, in contrast, that the d-wave outcome of spin-fluctuation modelling constitutes one of its affirmative attributes. Superconducting pair symmetry is transmitted through the range of pair coupling, and with spin coupling the nearest-neighbour axial Cu–Cu effects are dominant. However in the present negative-U model we likewise base the source of pair coupling upon an axially oriented short-range interaction: the negative-U electron pairing effect is not 'on site', but 'on coordination unit'. It is the elimination of the Cu–O antibonding interaction that drives the pairing of the electrons which source it. Accordingly the pair potential employed hitherto within the BCS formalism, namely a δ-function at $r = 0$ (r being the separation of the two pairing quasiparticles), should at least be replaced by a δ-function with $r = a_0/2$, the Cu–O basal bond length. Perhaps we might be

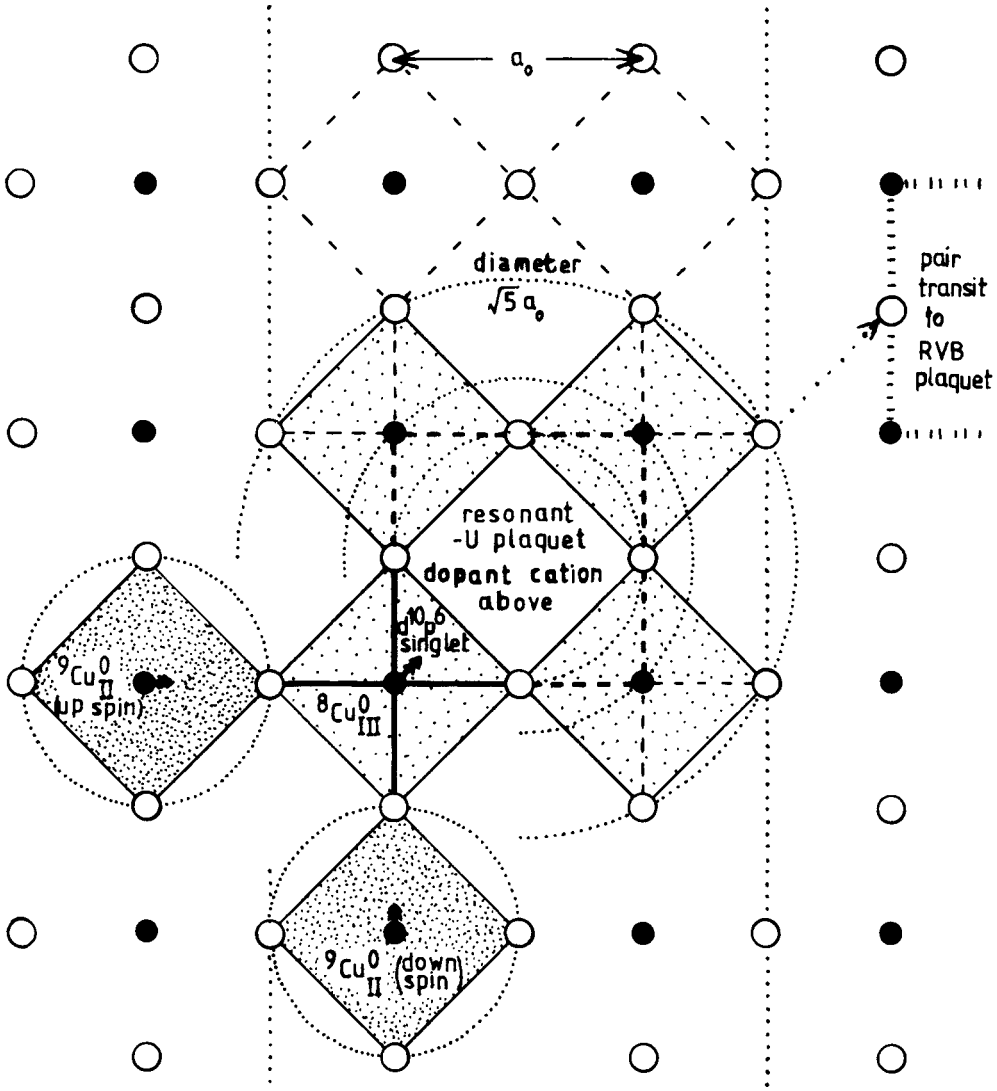

Figure 4. Segment of stripe phase domain wall showing $\sqrt{5}\ a_0$ diameter patch covering four coordination units around substituent doping centre where the Madelung potential is strongly augmented and the inward double-loading fluctuation $^{10}Cu^{2-}_{III}$ is able to acquire negative-U character.

somewhat more generous than this in view of the high Coulomb repulsion of the two electrons within a pair and the virtually unretarded nature of the interaction. Following my stripe phase and dopant modelling of earlier works, we observe from figure 4 that, when we choose to let one substituent counter-ion affect all four nearest-neighbour coordination units, the symmetrized patch over which the valence is augmented and negative-U pairing promoted could take a diameter of as much as $\sqrt{5}a_0$. This question of the pairing potential range is one currently being investigated by Quintanilla and Gyorffy [53].

4. A fresh look at the 12-point analysis of Wilson (1987, 1988) [1]: why HTSC is unique to these cuprates

By way of summary it would here be of value to return to the fundamental question raised in 1987—'why square-planar, layered, mixed-valent, cuprates?'. This will be answered first briefly and then by re-inspection in some detail of the original 12-point introduction to Wilson (1987, 1988) [1]:

(a) What cuprates introduce, even to an oxide, is a very substantial amount of p/d hybridization due to the proximity of d-shell closure. What however really singles out these cuprate compounds for HTSC is the potential for fluctuationally sampling shell closure itself.
(b) Without the mixed-valent substitution copper oxides universally are not metallic but Mott insulating—and to some considerable pressure. To secure HTSC behaviour it is, note, necessary for the mixed valence to be II/III, and not II/I, in order for the shell-closure, double-occupancy, negative-U mechanism to function.
(c) The layered character of the compounds boosts the generalized susceptibilities toward electronic instability. Furthermore it sustains the occurrence of an extended saddle point in the band structure near the band centre (i.e. near E_F), the heavily p/d hybridized basal carriers restraining magnetic pair breaking through encouraging $S = 0$ behaviour at trivalent sites and supporting RVB spin coupling over the Cu_{II} subsystem.
(d) The square-planar coordination geometry orients the saddle point VHs in the Cu–O basal bond direction. What is more it associates the negative-U pairing with the maximally antibonding $\{\pi, \pi\}$ regions of k-space into which the carrier pairs initially proceed.

Let us take a fresh look now at the 12 points specified by Wilson (1987, 1988) [1].

4.1. 'Metallic' conduction

The HTSC systems, although delocalized, have to be sufficiently close to localization for a local pairing mechanism not to be screened out. Already by $x = 0.20$ the materials are so metallized that it would seem quite unreasonable to seek a lattice polaronic interpretation of the superconductivity [13]. The corresponding mixed-valent nickelates etc are far too localized to support superconductivity, not only because they lack the basic conductivity but also because their magnetism is unquenched.

4.2. Jahn–Teller distortion

This effect, tied here to the d^9 site of the Cu_{II} subsystem, aids greatly in upholding the two-subsystem nature of the HTSC materials and, in particular, a negative-U option that is well defined as regards local double-loading. The strong local Jahn–Teller distortion assists moreover in organizing stripe phase formation (Wilson 1998) [1].

4.3. Secondary distortions

Most of the secondary distortions so widespread in these materials (e.g. LTO and LTT in LBCO) are structural accommodations to lattice mismatch between the CuO_2 layers and the so-called 'charge reservoir' layers. The apical Jahn–Teller elongated Cu–O bond of the Cu_{II} coordination units stands as a link between these structural segments. Even for YBCO the crucial CuO_2 'planes' emerge as not being perfectly flat. It has been stated that the materials holding the flattest planes attain the highest T_c. I do not believe that such a uniquely structural formulation can be the determining factor here. The J–T distortion plays an important part in

securing as short as possible a basal Cu–O bond, and thereby in establishing the non-spin-pair-breaking circumstances over both Cu subsystems. It is apparent that such Cu–O basal bond compression likewise is the benefit being conferred by insertion of extra fourfold coordinated CuO_2 layers in steadily advancing T_c through the initial part of sequences such as Hg-1201 (T_c = 97 K; Cu–O_b = 1.941 Å), Hg-1212 (T_c = 127 K; Cu–O_b = 1.926 Å), Hg-1223 (T_c = 133 K; Cu–O_b = 1.925 Å) [54]. To this extent I agree with the basic analysis offered by Muroi in figure 1 of [55].

4.4. Anderson localization

With such strongly defined two-subsystem behaviour it is remarkable that not more attention has been paid to the localizing effects of the inherent disorder, both directly on the quasiparticles and on the incipient pair behaviour. Much of the marginal behaviour of the Fermi liquid arising in the vicinity of the saddle points appears to be instigated in this way. While events just above T_c do not really appear like standard pre-pairing, as the rather limited critical fluctuation range $\sim$1 K would endorse [15], very significant local phase coherence effects in the 'para-conductivity' and 'para-susceptibility' and GHz conductivity remain very evident to $\Delta T/T_c \sim +0.15$, even for good quality samples [56]. Complementary to this, persisting tendencies to inhibited transport remain manifest below $T_c(H = 0)$ in the very-high-field experiments of Ando *et al* [57], as well as in what is detected by STM *within* individual flux vortices at much lower field strength [58]. It is rather ironic that Anderson himself chooses not to interpret the marked temperature variation of the Hall coefficient in this simpler fashion [59].

4.5. Low dimensionality

It is evident that the very poor c-axis conductivity of BSCCO-2212 is no bar to its excellent performance as a superconductor. Indeed even after being intercalated with iodine or organic complexes [60] the superconductivity is very little modified (just as was the case much earlier with the 2H-TaS_2 family [61]). c-axis interconnectivity would appear not to be a feature around which to develop an HTSC mechanism [59]. What the extreme anisotropy does lead to is a further weakening in antiferromagnetic order, while augmenting Anderson localization within the basal plane. In general it encourages Fermi liquid instabilities.

4.6. Fermi surface nesting

As the susceptibilities toward spin and charge density wave formation are built up, systems can bootstrap so that the Fermi surface geometry is modified towards greater instability [34]. The unstable regions in the present case are around the M points in the parent tetragonal zone. ARPES results indicate how the saddle-point dispersion of the F.S. geometry becomes much extended in the ΓM directions [33]. To the extent that negative-U behaviour is related to charge disproportionation the HTSC systems are more susceptible to charge ordering than to spin ordering. This becomes evident in the incipient stripe phase formation, where the charge spotting in the incommensurate neutron scattering data is seen at temperatures somewhat above those for spin spotting [9, 62]. It is my opinion, expressed in the stripe phase figures of Wilson (1998) and Wilson and Zahrir (1997) [1], that one must not however over-emphasize Fermi surface driven ordering in these systems. The stoichiometric count alone is sufficient to generate the structures drawn by Wilson (1998) and Wilson and Zahrir (1997) [1], without invoking k-space nesting. Remember in these 'marginal' mixed-valent metals the Fermi surface is poorly defined, especially at the saddle points, and the nesting characteristics are not exceptional.

4.7. Density wave states

All density wave states, especially SDWs, are seen as being in direct competition with the superconductive ground state option; witness the behaviour of 2H-$NbSe_2$ versus that of 2H-$TaSe_2$ and also of $NbSe_3$ [26].

4.8. Reduced moment magnetic order

It is clear from all sides that magnetic excitation is as detrimental to HTSC as it is to standard superconductivity. Clearly it is beneficial in the Mott-insulating parent materials that we are dealing with $S = \frac{1}{2}$ spin systems; quantum effects there indeed are able to diminish the site moment still lower to $\sim 0.6\ \mu_B$ [63]. In the substituted systems anything which acts to encourage Cu site moment retention has an adverse effect upon T_c. Prime examples of this are the effect of f^1Pr^{4+} [64] and $d^{10}Zn^{2+}$ [65] insertion. The particular energetics of these two elements and of the defect chemistry with which they are associated project magnetic activity into the basal CuO_2 plane, which becomes severely pair breaking. f^1Pr^{4+} appears to be present in a majority of $PrBa_2Cu_3O_7$ samples by virtue of the cross-substitution of Pr onto the Ba sites along with some incorporation of local excess of oxygen. The application of pressure and/or an enforced reduction in the oxygen content are able to prevent this, however, and thereby to introduce standard $RBCO_7$ superconductive behaviour. In a converse manner when weak magnetic order re-emerges in LBCO at $x = \frac{1}{8}$ HTSC is dramatically lost. There the remarkable oscillation near $x = \frac{1}{8}$ in the isotope effect upon T_c [66] should warn one though how inappropriate it is to consider spin effects in isolation from charge and lattice effects.

4.9. Non-stoichiometry

The non-stoichiometry is, as already noted, the route to metallicity in these systems, so close to the Mott transition. It leads to (and indeed helps via its disordering effects to preserve) the required two-subsystem behaviour upon which the present HTSC mechanism rests. Anion and cation substitutents are equally effective in generating HTSC, although it is evident that metal ion substitution is normally the simpler option both structurally and electronically (Farbod *et al* 2000, Ryder *et al* 1991) [1]. Excess oxygen and fluorine atoms prove unusually mobile in these materials to quite low temperature and that can create some awkward problems of detail. Nonetheless the striking feature as regards the HTSC phenomenon itself is that it is remarkably independent of detail of this type. This fact is well expressed by the empirical relations formulated by Presland *et al* [30] and Obertelli *et al* [67]. What really matters is simply the carrier count injected by the non-stoichiometry. Non-stoichiometric disorder additionally contributes to deterring any tendency to charge disproportionation and the emergence of some semiconducting ground state.

4.10. Non-rigid-band doping

As we have noted it is not possible to dope a Mott insulator in the manner of a semiconductor. Even for a non-T.M. system such as (Ga/In)As there actually is a remarkable degree of local structural disorder [68], not immediately apparent in the electronic properties. When dealing with strong CDW formation in 5d 1T-(Ta/Ti)S_2 [26, 69] it quickly became apparent that the events there did not rest entirely upon a well formed band structure, but upon more local interactions also. In the cuprate systems the gradual disappearance of such local response at high doping sees the disappearance of HTSC.

4.11. Rigid lattice with potential for M–M bonding

Towards the low-doping d^9 end of the HTSC regime it clearly is essential to suppress structured magnetism before it can lead to suppression of the superconductivity. We have used the concept of RVB introduced by Anderson [6] and developed by others [70] in order to effect this. This method of $S = \frac{1}{2}$ spin containment is plainly current in d^1 CaV_4O_9, where the crystal structure lends itself to square plaquet formation [71]. We have suggested it earlier to be source too of the moment-less, undistorted, low-temperature condition seen in layered orthorhombic d^1 TiOCl and TiOBr [7]. A great many other d^1 compounds which are not over-delocalized, such as VO_2, Ti_2O_3 and NbI_4, support an insulating ground state that is generated by *static* M–M bond formation [72]. One advantage of being currently at d^9 rather than d^1 is that we are dealing with states of antibonding e_g symmetry and not t_{2g} states. With the latter the orbitals often are able directly to interact, dimerizing cation centres. With e_g orbital geometry, M–M interaction usually is not direct, but mediated through a coordinating ligand. In those circumstances the lattice becomes much more resistant to deformation and RVB can come more readily to replace M–M dimerization as favoured ground state option. Several people have gone hunting for a reciprocal behaviour between d^1 and d^9 without recognizing that the crystalline geometries of the two orbital states in question are fundamentally different in their relation to the local coordination structure. An added distinction between the d^1 and d^9 conditions is that for the former E_F is close to empty band states, while with the latter it is close to filled states. There is not a symmetrical disposition here. This has its implications in that further option open to odd-number electronic systems—disproportionation.

4.12. Disproportionation

As we have already noted, disproportionation is in one way not a potential feature to be recommended when addressing superconductivity. It turns odd electron count systems into semiconductors; cf s^1 TlS or $BaBiO_3$, d^7 PtI_3, d^9 AuO. On the other hand, upon structurally and electronically frustrating such a system against cooperative disproportionation via a disordering of the local charge count, it becomes possible, as in $(Ba/K)BiO_3$, to conserve one very desirable aspect of such systems. This is their ability preferentially to entertain double occupancy of an orbital, able under sub-shell or full-shell closure to confer a superior stability. With $BaBiO_3$ we have the 'lone pair' s^2 condition (and s^0); with PtI_3 it is the low-spin t_{2g}^6 subset plus its square-planar d^8 complement. No such conferred state stabilization is potentially greater than that generated by full shell closure at d^{10}. In AuO however the d^{10} shell closure there defines statically (i.e. structurally) only a *uni*valent Au site. Where shell closure becomes of such crucial benefit to the mixed-valent cuprates in promoting HTSC is that it occurs now as an intersite double-loading charge fluctuation ($^{10}Cu^{2-}_{III}$) at sites which are being driven towards *tri*valency by the counter-ion doping. It is in this enhanced local Madelung potential that the effects of shell closure become so marked—a negative U of several eV in magnitude, as in figure 2. The effect of valence change upon the energetics of the various states, static and fluctuational, has been presented in figure 3 of Wilson (1988) [1], constructed from the related figure 7 of [73]. In the latter figure all the d states were incorporated, not just the $d_{x^2-y^2}\sigma^*$ state of immediate concern to the HTSC cuprates and final d-shell closure focused upon in Wilson (1987, 1988) [1]. Figure 5 recaps this state of affairs.

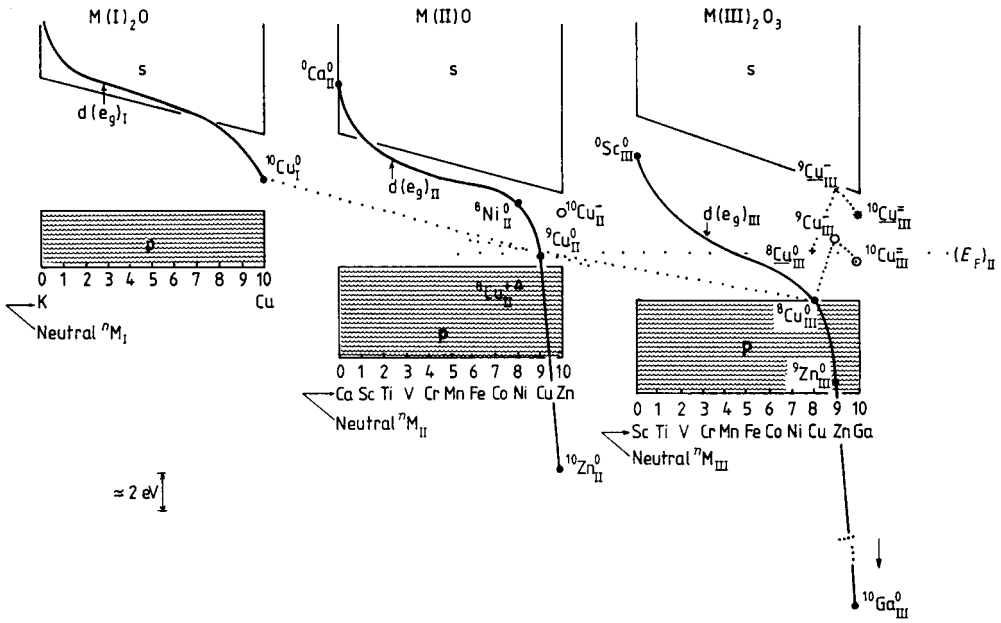

Figure 5. A slight refinement of a figure from Wilson (1987, 1988) [1] illustrating the relative positions of the states of interest in mono-, di- and tri-valent 3d oxides. Of the d bands only the uppermost pd(e_g)σ^* band, most relevant to HTSC work, is shown—for a fuller version see figure 7(b) of [73]. With increasing cation valence the main valence p-band position drops with decrease in cation radius in the increased Madelung potential and widens due to the greater degree of covalent mixing which ensues. The location of the e_g^* band skews downwards strongly with increasing valence, following the decrease in state radial expectation value. In neutral $^{10}Ga^0_{III}$ the closed d shell has dropped to 18 eV below the top of the non-bonding p-state reference point. This allows the doubly loaded fluctuational state $^{10}Cu^{2-}_{III}$ to achieve negative-U character and to end up in near-resonance with E_F in the mixed-valent cuprates.

5. Some neutron and NQR work in the light of the above approach

Nowhere are results more fragmented and confused than in neutron scattering, which is regrettable since neutron work, with its ability to probe action over k-space as well as scattering energy, is potentially most favourably placed to resolve matters. One serious problem is that because large crystals are required neutron work has been almost entirely limited to the LSCO, LCO+ and YBCO-123 systems. A crucial concern with neutron data, as with so much other HTSC data, is to make proper assignment of the detailed results to superconducting as distinct from spin gap phenomena. Neutron scattering by electrons refers essentially to spin scattering. One must however not desire to make that synonymous with 'magnetic scattering' and still less with antiferromagnetic spin-wave magnon scattering. In LSCO residual magnon scattering *is* evident, but only at energies above 25 meV [74]. At lower energies one is involved with (i) spin gapping under RVB formation, (ii) the association of this with IC stripe phase charge and thereby spin segregation, and (iii) spin-triplet excitation of the singlet boson pairs (which exist in small numbers to well above T_c). Such matters are raised in the recent paper on LSCO by Lake *et al* [75], but patently lack there any clear resolution. I would like here to advance the view presented in figure 6 as a basis for interpretation of the various neutron results. Note the IC peaks recorded in fact display a 'long' coherence length—one compatible with the charge domain size (∼30 Å) (Wilson and Zahrir 1997) [1].

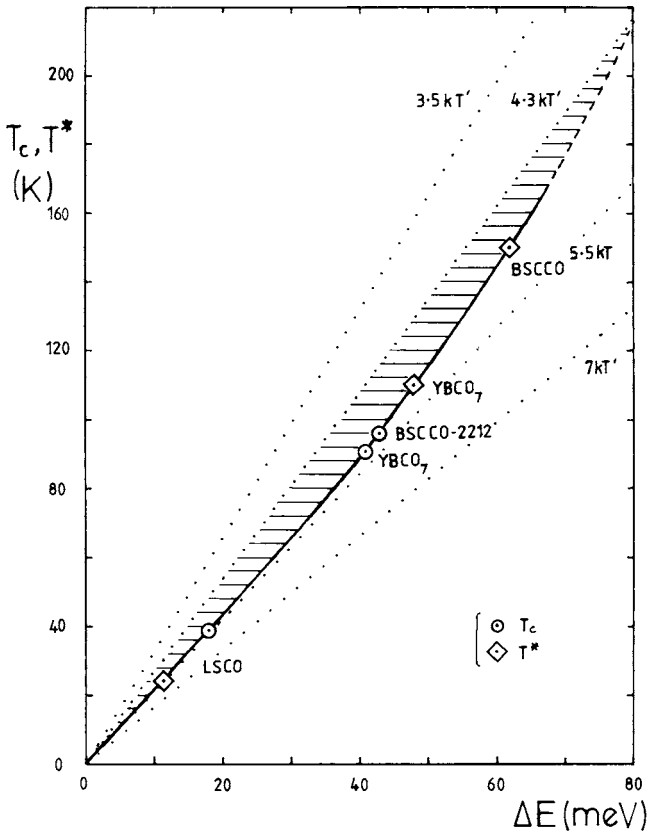

Figure 6. Plot of T_c and $T^{*\prime}$ against the corresponding excitation energies, extracted mainly from neutron work (see text). The six data points for optimally doped BSCCO-2212, YBCO-123 and LSCO-214 appear to lie on a single slow curve. The latter is bounded at small T by the strong-coupling line $2\Delta/kT \sim 5.5$, while at high characteristic temperatures it swings round towards the weak-coupling mean-field d-wave symmetry value of 4.3. In the case of LSCO note that T^*, the temperature of complete spin gapping, has become less than T_c.

The instrumentally narrow 41 meV resonance peak appearing in $YBCO_7$ below $\sim T_c$ around points $\{\pi, \pi, \zeta'\}$ [45] is perceived as noted above to be the spin triplet energy of layer-separated pairings, and is as such very close to the maximum superconducting gap energy (Wilson and Zahrir 1997 [1], section 8.5). That accords with the dielectric changes observed at this energy ($\equiv$330 cm^{-1}) in optical phonon work [21, 22, 76]. The corresponding energy for BSCCO-2212 is 43 meV [44]. These energies place events in the moderately strong-coupling regime, given a (dominantly) d-wave interaction, *viz.*, $2\Delta(0)^{max}/kT_c \approx 5.2$, as compared with 4.3 now for mean-field behaviour. We have taken here T_c for well-formed BSCCO-2212 at optimal doping to be 96 K [77]. For $YBCO_7$ the spin-gap edge energy (of the Cu_{II} subsystem), in evidence in figure 3(c) of Dai *et al* (1996) [45], is read as being 50 meV. This I have associated with a spin gap 'completion' temperature $T^{*\prime} \approx 110$ K, as is suggested by spin–spin coupling experiments on $REBa_2Cu_3O_7$ [78] and also by electrical noise measurements [79]. For BSCCO the spin gap opened is considerably higher, and experiment would support a 0 K gap energy of 62 meV in conjunction with a spin gap completion temperature $\approx$150 K (see figure 2 in [80] and figure 6 in [81] respectively). (Tunnelling results from BSCCO are

so variable in all aspects that I cannot believe most as yet relate to what is claimed [47, 82].) Extrapolating the line through the four points now inserted on figure 6 back towards the origin takes us into the region occupied by the LSCO data [45, 75]. With LSCO it is not unreasonable that the order of the above two gaps becomes inverted (i.e. the Cu_{II} spin gap attainment occurs below the superconducting T_c). Such inversion is naturally related to the small T_c value for this more magnetic, more ionic system (Wilson 1994a) [1]. The feature with which the paper on LSCO from Lake *et al* [75] deals mostly is then not the pair spin-triplet gap (equivalent to the 41 meV peak in $YBa_2Cu_3O_7$), but rather the RVB spin gap of the Cu_{II} subsystem. In view of its d-wave nature I would prefer to locate the latter energy not at the edge mid-point energy of 6.8 meV (as was done in [75]) but to use the edge top energy of 11.4 meV. This stands then as a counterpart to the 50 meV reading made for $YBCO_7$ (Dai *et al* 1996) [45]. For the LSCO case that would leave the very strong broad peak at 18 meV as marking the spin-triplet energy, equivalent to the sharp 41 meV peak in $YBCO_7$. The precise spectral form in the final state for single layer LSCO inevitably must be appreciably different from that for bilayer YBCO and BSCCO (for which $k_z = \zeta'$, with ζ' corresponding to the intra-bilayer spacing). The 18 meV feature indeed presents the appropriate behaviour regarding superconductivity, which the work of Lake *et al* [75] demonstrates the 11.4/6.7 meV edge not to possess. The latter low-energy edge is manifestly related to enhancement of the incommensurate stripe phase domain order coming with complete development of the spin gap and RVB somewhere below T_c. By 5 K the IC peaks clearly have become significantly sharper and stronger.

Because it would appear from figure 6 that the five points already in place fall there upon a common curve associated with strong-coupling behaviour, we observe that for the LSCO spin gap one can anticipate a characteristic gap opening temperature near 25 K to partner the final (0 K) gap energy of 11.4 meV. By LSCO the points above appear constrained to a $2\Delta(0)/kT$ limit $\approx$5.5. This ratio drops gradually to the d-wave mean-field value of 4.3 upon reaching $T' \sim 220$ K, a temperature generally accepted as marking the upper limit to 'HTSC' phenomena, even under pressure.

What evidence is there for the above synthesis—in particular for the inferred magnetic change in optimally doped LSCO near 25 K? Upon investigation a strong feature already has in fact been detected at 27 K by ultrasonic attenuation, employing a good TSFZ crystal with a T_c of 37 K [83]. The feature displays the frequency characteristics of a magnetic relaxation process. Moreover, from sound velocity measurements made in a magnetic field [84] one is able by an analysis of the flux flow to extract an $H \parallel c$ pinning energy of 11 meV, with an onset to pinning at the indicated temperature. μSR-determined λ_{ab} data show similar deviance, though not quite so strongly, within data obtained at lower fields (see figure 1(a) in [85]). The event around 25 K accordingly would appear magnetic in nature, and it clearly deserves further investigation now by repeating the neutron work at intermediate temperatures. All sorts of raised values currently abound for 'T^*' in LSCO and family (e.g. in C_v work, note figure 4 of [86]). Break temperatures up in the vicinity of 60–80 K are clearly due however to the LTO–LTT transition and to IC stripe phase fluctuations, while effects around 200 K arise from the HTT–LTO transition and from oxygen migration. The systematics of figure 6 make sense in the light of the discussion provided by Wilson and Zahrir (1997) and Wilson (1994a) [1], and will form the basis upon which we shall proceed in due course to examine some recent theoretical works, holding throughout to our negative-U understanding of HTSC.

In progressively underdoped, less delocalized samples than the above, we expect T_{sc} and $T^{*\prime}$ to converge steadily to zero, reflecting the growth in standard antiferromagnetic correlations in such systems, for each at a rate appropriate to its own particular level of covalent hybridization. Figure 7(a) indicates how we anticipate $T^{*\prime}$ and $2\Delta^{*\prime}$ to vary as a function of the carrier content p across the above three systems, LSCO, YBCO-123 and BSCCO-2212, in

order of steadily increasing covalence. In figure 7(b) the $2\Delta_{sc}$ plots have provisionally been assigned the same parabolic variation in p as that followed by the corresponding $T_{sc}(p)$ plot. In consequence the $2\Delta_{sc}/kT_{sc}$ ratio will automatically remain fixed for all p. The strongly contrasting $2\Delta^{*\prime}/kT^{*\prime}$ ratios are shown plotted against p in figure 7(c). There the three curves reveal for the spin gap behaviour a very rapid movement with p (using the input of figures 7(a) and (b)). This ratio becomes systematically reduced as the counter-ion ionicity is diminished. It ought to be noted that only at optimal doping do the two $2\Delta/kT'$ ratios become closely similar between pairs of superconducting and spin gap plots. The T_c curves superimposed on figure 7(c) make use of this to allow better comparison between the two phenomena. While the LSCO panel acquires the general appearance of the figure deduced by Loram and others [15] note it now is for $2\Delta^{*\prime}/kT^{*\prime}$ and not $2\Delta^{*}$. The $2\Delta^{*\prime}(p)$ 0 K values that we have employed can themselves be seen in figure 7(b), where they are given on the right hand scale converted to equivalent temperatures. Selection of these 0 K spin gap values was governed by the full compass of the neutron data. For the LSCO system they as noted bear remarkably close agreement with the $2\Delta^{*}(p)$ values extracted from specific heat data by Loram *et al* [15]. That however is not the case for YBCO. Perhaps the chains disturb there the sensitive specific heat analysis—our own systematics would appear fine and not too contrived. Remember throughout the above that we are dealing with the final opening up of the RVB spin gap and *not* with the initial deviation from standard SRO antiferromagnetic coupling. The latter of course sets in at considerably higher temperatures, as oxygen spin–lattice nmr relaxation in particular records.

Often it is said that it is difficult to reconcile the nmr and neutron data. However it has to be recalled that the nmr/nqr probe is ultra-sensitive to the local structure and that the latter is strongly inhomogeneous in the mixed-valent HTSC samples. The local site nqr behaviour (governed by the local electric field gradient) is, it is clear, sensitive not only to the static dopant ion sitings but also in particular to the locations within the CuO_2 array of the inserted holes themselves (and expressly their segregation into the stripes). We noted above that in fact a sizeable fraction of the holes become localized on a significant time scale (say 10^{-6} s). Some years ago Martin [87] using an embedded small-cluster Hartree–Fock technique (and employing a comprehensive cluster basis set in the manner of Wachters) demonstrated how a much broadened strongly multi-signal Cu nqr response should follow. Such a signal indeed was in evidence in the existing data [2, 35]. Originally Yoshimura *et al* attributed the strong satellite peak they had observed accompanying the main peak in LSCO (and subsequently in LCO+ too) to those Cu sites immediately contiguous to a substituent ion (namely an Sr^{2+} or interstitial O^{2-}): this was in view of the satellite intensity being $\propto x$ (or p). Martin showed that actually a much greater effect, by an order of magnitude and more, is to be expected on site in the presence of a hole carrier itself. For that circumstance the ^{63}Cu nqr frequency is calculated to shift hugely from around 35 MHz to 90 MHz as the formal on-site electron count, if taken to be entirely localized, becomes changed from d^9 to d^8 (see section 1). By contrast at optimal doping the *observed* shifts to principal peak and satellite are <5 MHz for LSCO and LCO+, and must hence only in part sense any such localization. Tellingly too the observed main peak shift is identical between these two systems, indicating that the shifts are not dictated by the actual manner of introduction of the charge. The calculated results would suggest that $\sim$70% of the inserted charges have in fact to be highly mobile (at 300 K for $x = 0.15$), or, conversely, that only some 30% can actually be localized on the NQR time scale ~ 1 μs. It seems likely that the distinction here between 'localized' and 'delocalized' holes is set by whether a hole finds itself by chance in the same unit cell as a hole donor ion nucleus or not. For a crossed stripe array at $x = 0.166$ this would result in a fraction $\{2(\frac{1}{6}) - \varepsilon\}$ of the holes appearing localized; the ε, included here to remove double counting in the 2D stripe array, is still small at $x = \frac{1}{6}$. The above fraction agrees quite closely with

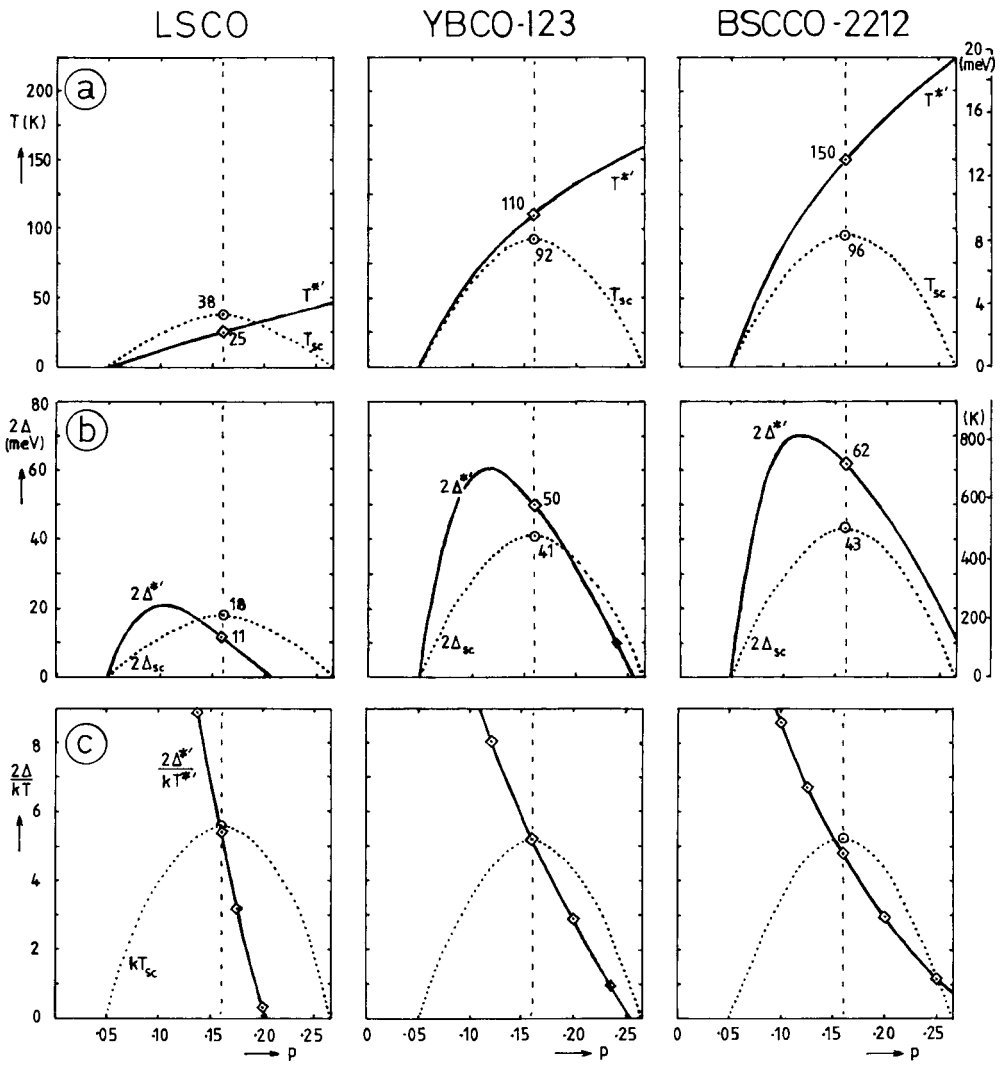

Figure 7. (a) The customary parabolic form of $T_c(p)$ for LSCO, YBCO-123 and BSCCO-2212 shown in conjunction with the proposed interpretation of the RVB gap completion temperatures $T^{*\prime}$ (on cooling), as construed from the neutron data for the optimally doped materials. (b) Matching plots for the respective maximum gap values Δ_{sc} and $\Delta^{*\prime}$ versus p, again based around the neutron data. $\Delta_{sc}(p)$ provisionally is given the same parabolic form about $p = 0.16$ as $T_c(p)$. By contrast the $\Delta^{*\prime}(p)$ graphs are very skewed toward the low-p, magnetic direction. The gapped area on the plots becomes greater the greater the covalency of the system. (c) $2\Delta^{*\prime}/kT^{*\prime}$ for the completion of the spin gap is shown plotted against p. These plots are displayed on a background of $T_c(p)$ anchored to the maximal point, where $2\Delta/kT$ happens to be closely similar for both the RVB and superconducting gaps (see figure 6).

the experimentally deduced fraction of 'localized' holes being about 30%. Only this subset of holes leads to an upward shift in the main peak frequency of sizeable magnitude. The satellite peak likewise shifts to higher frequency with p (though only at half the rate). The satellite peak itself is ascertained by Martin to issue from those d^9 sites which are nearest neighbour to a *localized* d^8 site hole. In accord with this the observed relative intensity of the satellite

grows only at roughly the rate of doping and not at four times that rate as might otherwise have been expected.

Because the detailed microstructure of the HTSC cuprates is of such importance to interpreting NMR and neutron work—and indeed to the HTSC mechanism itself, whether of stripe phase form [11] or my own chemical negative-U interpretation—it becomes desirable to make closer examination of Martin's results [87]. Hitherto these have been rather overlooked, and that is a pity, because of all techniques nqr is least intrusive, besides being highly sensitive to the local environment—of primary import to a superconducting system for which ξ is pointedly so short. In the first line of figure 8 are inserted the calculated positions (in MHz) of the ^{63}Cu NQR main peak for entirely *localized* d^9 and d^8 site loadings. These evaluations have been made with the cluster bonds fixed at the lengths appropriate to $x = 0.15$, a constraint which will be corrected for below. (Line 2 of figure 8 indicates that the calculation is somewhat overstating the actual d^9 frequency by about 5 MHz.) Upon making a linear interpolation in line 1, the main peak for optimally doped material might, if localized, be expected to occur shifted up by 8 MHz from the fully divalent position. Line 2 reveals the experimental shift however to be only 2.1 MHz. This would imply, as was discussed above, that only 26% of the holes are apparently effective, i.e. localized. The latter figure needs correcting somewhat now for the lattice parameter adjustment. Recall it is the field gradient change that controls the nqr signal; i.e. there are both charge and geometric components to the peak shift rate. From the experiment the full incremental shift from di- to tri-valence for the main peak would extrapolate as being 14 MHz (see the lower plot in the inset to figure 2 of [87]). Requiring next to be added to this is a shift of 3 MHz coming from the lattice contraction from d^9 to d^8. The latter value has been evaluated by use of $(\Delta\nu/\Delta p) \equiv (\Delta\nu/\Delta R_{Cu-O})(\Delta R_{Cu-O}/\Delta p)$. Here $(\Delta\nu/\Delta R_{Cu-O})$ was determined by Martin as being -91 MHz Å^{-1}, while $(\Delta R_{Cu-O}/\Delta p)$ can be extracted from existing crystallographic data as -0.035 Å e^{-1}. The unit charge increment to compare with line 1 in figure 8 accordingly will be +17 MHz. The entirely localized evaluations in line 1 yielded a value of 53.4 MHz. This implies, as was indicated above, that only 17/53.4 or 32% of the holes are 'effective' here, i.e. are localized on the NQR time-scale. It would be interesting to find out whether the temperature dependence of this fraction might be determinable. Note the above numbers are not quite as given by Martin in [87] because the crystallographic data have since been upgraded. In affirmation of these calculations it might be recorded that the observed shift of the satellite relative to the main peak at $x = 0.15$, namely 2.8 MHz, matches closely Martin's calculated value of 2.7 MHz—once that signal is taken as coming from a d^9 site *next to* a localized d^8.

6. Some features of our negative-U approach to be sought out in current theory

Let us recap on what was presented in figure 3. Good quasiparticles (like 1 and 2) are very readily drawn off into the scattering sinks around the saddle points. From there as very heavy particles (like 5 and 6) they are able to be transmuted into pair form (7) with a net crystal momentum out in the first instance near $(\pi, \pi)1/a$. Immediately however, because of the equivalence in real space to local shell closure of what is effected in these heavy spin-0 composite units, the latter become taken back energy-wise to reside near-resonantly with E_F under a negative $U_{eff} \approx -1.5$ eV per electron of the pair. If now we assign to the two electrons within each local pair identical linear velocities and momenta, then, in contrast to the equal and opposite crystal momenta of the customary retarded interaction Cooper pair, the individual electron momenta become $\approx(\pi/2, \pi/2)1/a$, i.e. somewhat in advance of the single-electron Fermi sea in the (k, k)-direction. By T_c such pairs must form faster than they can relax and very rapidly build up a sizeable population. With the Bose condensation of pairs that ensues, their

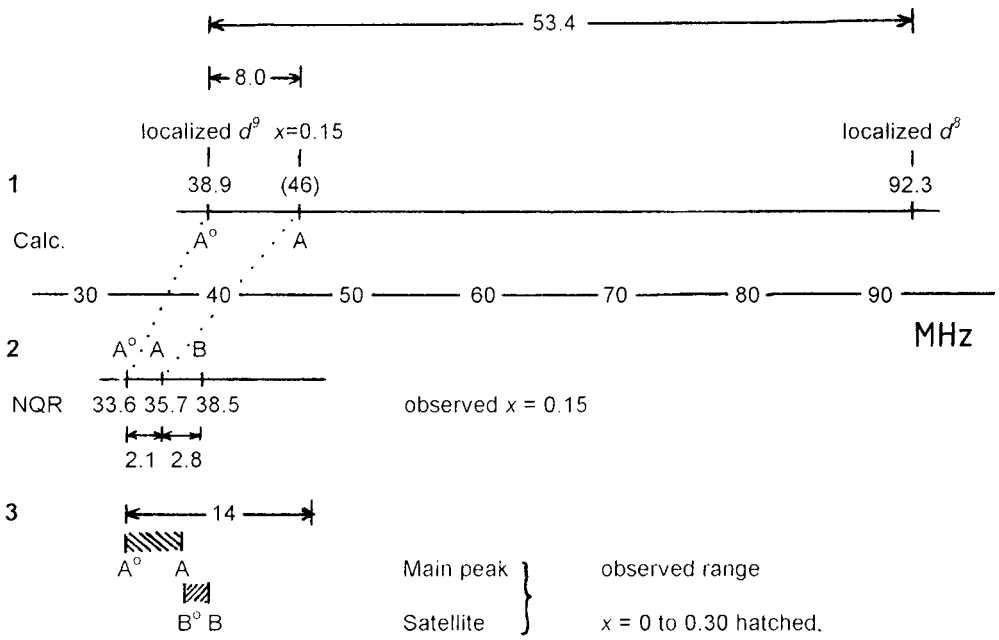

Figure 8. Theoretical results of Martin [87] compared with the experimental NQR data from LSCO and LCO+. Line 1 shows the peak positions as calculated on a localized basis, while lines 2 and 3 compare the observed main (A) and satellite (B) peak positions.

crystal momenta within the coherent many-body condition at low temperatures will approach zero. The establishment of superconducting phase coherence sees the individual carrier energy pass below E_F or μ by the effective superconducting order parameter energy, $\Delta(\theta, T)$. In the above scenario note that although the *pair's* crystal momentum is to begin with preferentially in the $\{k, k\}$-directions, the electrons being abstracted into the pairs come from the $\{\pi, 0\}$ saddle points. It is in the latter regions that the quasiparticles effectively become most stabilized below the Fermi energy/chemical potential by the amount Δ^{max}. This 'gapping' energy is, at first sight, extractable from ARPES data taken below T_c, by seeking to track the changes seen near E_F out into the saddle point regions. Ordinary optical measurements do not couple in strongly enough to register either this energy nor indeed 2Δ. One place where the full 2Δ pair excitation is closely recorded is in the inelastic polarized neutron spin-flip scattering experiments introduced in section 5. Such excitations are of the paired quantum condensate itself. Recall that for $YBCO_7$ the much discussed 41 meV resonance peak is instrumentally narrow in excitation energy [45]; i.e. it relates to a condition that is rather long lived, little broadened by disorder or phonons. It represents the (interplanar) spin-triplet excitation for the paired condensate, and being essentially of a local negative-U pair will effectively mark the latter's disruption. The 41 meV input sees a return of two electrons from the condensate back to E_F in the saddles. The net momentum supply from the neutron needed to accomplish this per extracted pair is, note, the full ΓX complement π, π. Thus the mixed boson–fermion scenario, where the electronic system creates its own bosons, is very significantly different from standard superconductivity—or, rather, the long-standing view that the BCS treatment has offered of typical s-wave superconductors. Because HTSC clearly involves carrier pairing, as was demonstrated early on through SQUID [88] and Bitter pattern [89] results, and because of the rather general formulation to customary Ginzburg–Landau prescriptions [90], it has not

always been appreciated how differently the HTSC systems might in detail comport themselves as compared with standard long-coherence-length s-wave superconductors.

One very big difference in the above sketched scenario is that the pairs are not Cooper pairs in that they are not composed of $+k$ and $-k$ partners. The present strongly coupled quasiparticle partners initially have both fermionic wavevectors (and velocites) that are virtually at right angles to each other. The bosonic condensate displays ultimately the same strong $d_{x^2-y^2}$ local gapping anisotropy as is shown by the magnetic pseudogapping. The pair coupling process is not retarded, but occurs directly into the heavy composite local bosons. Differently again, this pairing is precipitated via action in the very direction for which quasiparticle Fermi surface gapping is weakest, and *vice versa*. We reach the odd effect of the neutron spin-flip assessment of $2\Delta^{max}$ being obtained through neutron spin scattering at momentum transfer π, π, while ARPES makes its single-electron assessment Δ^{max} (or rather of $3\Delta^{max}$—see below) of the superconducting Fermionic gap by excitation in the vicinity of the saddle points $\{\pi, 0\}$. In the neutron experiment the electrons of the decondensed broken pair are returned simultaneously to nearest-neighbour saddles, spin parallel. It is a highly significant and usually overlooked observation that while in YBCO the spin gap discussed in section 5 is detected as a diffraction rod up the q_z-axis, the resonance peak is restricted to $q_z = \zeta' = 2\pi/d$, d here being the z-axis spacing between the two coupled CuO_2 planes of a YBCO cell [91]. The RVB spin coupling renders all CuO_2 planes randomized towards magnetic z-axis scattering in relation to spin gap formation. By contrast the stacking of the charge stripe arrays in staggered fashion between the two layers involved leaves the spin-triplet excitation of the HTSC condensate imprinted in the above manner (misleadingly labelled 'acoustic' by Dai *et al*, and 'odd' by Keimer *et al*). The stripes are, remember, where the negative-U pair creation and destruction proceeds. This staggered stacking between the stripe arrays in successive layers is driven coulombically and by the strong c-axis Jahn–Teller distortion.

The strong π, π resonance above has nothing to do then with spin waves and magnetic ordering (specifically antiferromagnetism). The experimental peak is far too narrow in energy—at a stage where prior to condensation the system is highly disturbed. The peak's integrated spectral weight is furthermore far too small for it to relate to a uniform $S = \frac{1}{2}$ situation (see caption to figure 3 of Dai *et al* (1999) [91]). Where features of a magnetic origin actually do become sensed in the neutron spin scattering is with the four weak incommensurate inelastic scattering peaks sited at some distance about π, π [8, 92]. These, as was stated earlier, are of a coherence length to match the size of the stripe domains (∼35 Å). In figure 8 of Wilson (1998) [1] it was proposed that this magnetic scattering arises from spin cantings at the edges of the RVB-structured domains, as those arrays configure themselves in antiphase fashion across the domain walls. At the given high level of hole doping residual SRO AF coupling is of a still further reduced coherence length and contributes simply to the broad background under all the above scattering features.

It is appropriate at this point to clarify the relationship between the sharp initial peak seen in ARPES (and tunnelling spectroscopy) and the above resonant neutron scattering peak. Because the former was discovered first it inevitably became associated with 'Δ'. However it is the neutron experiment which directly accesses the condensate. A recent closer examination of the ARPES data has revealed that the initial peak is not actually a straightforward quasiparticle peak. Unlike the succeeding hump at 3Δ, it is a non-dispersing feature in k-space, recorded both well inside and indeed even well beyond the Fermi surface. Norman *et al* [93] have reasoned that this resolution-limited spectral peak must in fact result from a sharp step down in $\mathrm{Im}\Sigma$ at 2Δ (43 meV in optimally doped BSCCO-2212), along with the associated peak in $\mathrm{Re}\Sigma$. These are precisely the changes in the electronic self-energy to be anticipated as a consequence of the superconductive condensation being the product of direct electron–electron

interaction. Norman *et al* demonstrate that the little-dispersing initial spectral feature is the immediate outcome of this circumstance, as too is its observed spectral weight change over k-space. The best matching to the ARPES data emerges for $(2\Delta)_{sc} \approx 1.3\Delta_{ARPES\,pk}$ (where $\Delta_{ARPES} = 32$ meV for BSCCO). We can appreciate now why there has always been some mismatch between the 'Δ' values quoted from ARPES (and tunnelling) versus those obtained with certain other probes. In the present d-wave negative-U situation the measured 'gaps' are, it is evident, not always so immediately relatable to the order parameter gap as they are in standard s-wave BCS superconductors.

It is of considerable interest now in closing to identify some recent formal theoretical works [94–112] that might be re-slanted toward accommodation of the above expressed views. One fundamental flaw with the great majority of theoretical approaches is that they tie their attention solely to the pdσ^* $x^2 - y^2$ symmetry E_F-bearing band. At the very least, in order to incorporate adequately the bonding effects of fluctuational site loading change, one should incorporate the corresponding response of the deep-lying pdσ bonding partner. To embrace properly the crucial changes which are enfolded in figure 5 almost certainly will necessitate in fact including the entire set of outer s, p and d states from both Cu and O sublattices. Without the shell-closure effects implicated previously, with their resulting gross modification in state energies, it would appear there is no way in practice of encountering a negative-U circumstance. Only such bonding energy changes are of a magnitude sufficient to override the very sizeable Coulomb energies inescapable in these all but Mott-insulating materials. Without such input most current negative-U treatments inevitably fail to produce results displaying closely identifiable detail, and then fail to confine those results as restrictively to the II/III cuprates as experiment would demand.

In addition to the limited basis set employed, other persistent points of lack of contact with the experimental position are the need to recognize the intrinsic inhomogeneity of the materials and the appreciable local structural accommodation involved in site charge loading change, static and dynamic. Coulomb and Jahn–Teller contributions to the HTSC condition remain very strong, it being one so close to the Mott transition. With the advent of stripe phase diffraction the two-subsystem character is now happily more widely acknowledged.

I realize it is rather easy for a non-formal theorist to ask for such developments. Nonetheless for those at this point prepared to attempt something more adventurous it would seem that many among the formal works listed here would bear profitable extension along the directions indicated. In this, as was requested at the outset, one will have to keep a closer eye on the chemistry, directing one's focus consistently upon that central question 'Why only square-planar, II/III mixed-valent cuprates?'. It is only in the complex fusion of all the aspects relating to the HTSC materials—which so many currently are dealing with in isolation—that the highly restrictive character of the HTSC cuprate phenomenon can emerge. The answer is in the detail, and *in practice* without that detail HTSC would not exist. Only a theorist could at this juncture ask 'Why is T_c so low?': rather look to that very small window of opportunity which permits it to be so high.

References

[1] Farbod M, Giblin S, Bennett M and Wilson J A 2000 *J. Phys.: Condens. Matter* **12** 2043–52
Wilson J A and Farbod M 2000 *Supercond. Sci. Technol.* **13** 307–22
Wilson J A 2000 *J. Phys.: Condens. Matter* **12** 303–10
Wilson J A 1999 *Supercond. Sci. Technol.* **12** 649–53
Wilson J A 1998 *J. Phys.: Condens. Matter* **10** 3387–410
Wilson J A and Zahrir A 1997 *Rep. Prog. Phys.* **60** 941–1024
Wilson J A 1996 *J. Phys.: Condens. Matter* **9** 6061–8

Wilson J A 1994a *Physica* C **233** 332–48
Wilson J A 1994b *J. Supercond.* **7** 585
Ryder J, Midgley P A, Exley R, Beynon R J, Yates D L, Afalfiz L and Wilson J A 1991 *Physica* C **173** 9–24.
Wilson J A 1989 *Int. J. Mod. Phys.* B **3** 691–710
Wilson J A 1988 *J. Phys. C: Solid State Phys.* **21** 2067–102
Wilson J A 1987 *J. Phys. C: Solid State Phys.* **20** L911

[2] Yoshimura K, Imai T, Shimizu T, Ueda Y, Kosuge K and Yasuoka H 1989 *J. Phys. Soc. Japan* **58** 3057
Haase J, Curro N J, Stern R and Slichter C P 1998 *Phys. Rev. Lett.* **81** 1489
See also [35]

[3] Massidda S, Yu J, Freeman A J and Koelling D D 1987 *Phys. Lett.* A **122** 198
Massidda S, Yu J, Freeman A J and Koelling D D 1987 *Phys. Lett.* A **122** 203

[4] Bianconi A, Saini N L, Rosetti T, Lanzara A, Perali A, Missori M, Oyanagi Y, Yamaguchi H, Nishihara Y and Ha D H 1996 *Phys. Rev.* B **54** 12 018 (BSCCO)
Saini N L, Lanzara A, Oyanagi Y, Yamaguchi H, Oka K, Ito T and Bianconi A 1997 *Phys. Rev.* B **55** 12 759 (LSCO)

[5] Nakamura F, Goko T, Hori J, Uno Y, Kikugawa N and Fujita T 2000 *Phys. Rev.* B **61** 107
Locquet J P, Perret J, Fompeyrine J, Mächler E, Seo J W and Van Tendeloo G 1998 *Nature* **394** 453

[6] Anderson P W 1973 *Mater. Res. Bull.* **8** 153
Fazekas P and Anderson P W 1974 *Phil. Mag.* **30** 423

[7] Beynon R J and Wilson J A 1993 *J. Phys.: Condens. Matter* **5** 1983
Wilson J A, Maule C, Strange P and Tothill J N 1987 *J. Phys. C: Solid State Phys.* **20** 4159

[8] Shirane G, Birgeneau R J, Endoh Y, Gehring P, Kastner M A, Kitazawa K, Kojima H, Tanaka I, Thurston T R and Yamada K 1989 *Phys. Rev. Lett.* **63** 330
Cheong S-W, Aeppli G, Mason T E, Mook H, Hayden S M, Canfield P C, Fisk Z, Clausen K N and Martinez J L 1991 *Phys. Rev. Lett.* **67** 1791
Mason T E, Aeppli G, Hayden S M, Ramirez A P and Mook H 1993 *Phys. Rev. Lett.* **71** 919

[9] Niemöller T, Ichikawa N, Frello T, Hünnefeld H, Andersen N H, Uchida S, Schneider J R and Tranquada J M 1999 *Eur. Phys. J.* B **12** 509 ($(La/Nd/Sr)_2CuO_4$)
Kimura H *et al* 1999 *Phys. Rev.* B **59** 6517 (LSCO)

[10] Kleiner R *et al* 1996 *Phys. Rev. Lett.* **76** 2161
Tsuei C C and Kirtley J R 1997 *Physica* C **282–287** 4

[11] Emery V J and Kivelson S A 1999 *J. Low Temp. Phys.* **117** 189

[12] Bianconi A, Valetta A, Perali A and Saini N L 1996 *Physica* C **296** 269
Bianconi A, Valetta A, Perali A and Saini N L 1997 *Solid State Commun.* **102** 369

[13] Alexandrov A S and Mott N F 1995 *Polarons and Bipolarons* (Singapore: World Scientific)
Alexandrov A S and Kabanov V V 1999 *Phys. Rev.* B **59** 13 628
Ranninger J, Robin J M and Eschrig M 1995 *Phys. Rev. Lett.* **74** 4027
Ranninger J and Romano A 1998 *Phys. Rev. Lett.* **80** 5643

[14] Trivedi N and Randeria M 1995 *Phys. Rev. Lett.* **75** 315

[15] Loram J W, Mirza K A and Cooper J R 1998 *Research Review 1998 HTSC* ed W Y Liang (IRC, University of Cambridge) pp 77–97
Williams G V M, Tallon J L and Loram J W 1998 *Phys. Rev.* B **58** 15 053
Junod A 1996 *Studies in HTSC* vol 19, ed A V Narlikar (New York: Nova)

[16] Uemura Y J *et al* 1993 *Nature* **364** 605
Uemura Y J 1997 *Physica* C **282–7** 194

[17] Micnas R, Ranninger J and Robaszkiewicz S 1990 *Rev. Mod. Phys.* **62** 113

[18] Friedberg R and Lee T D 1989 *Phys. Lett.* **138** 423
Friedberg R and Lee T D 1989 *Phys. Rev.* B **40** 6745

[19] Norman M R, Ding H, Randeria M, Campuzano J C, Yokoya T, Takeuchi T, Mochiku T, Kadowaki K, Guptasarma P and Hinks D G 1998 *Nature* **392** 157
Ding H, Norman M R, Campzano J C, Randeria M, Bellman A F, Yokoya T, Takahashi T, Mochiku T and Kadowaki K 1996 *Phys. Rev.* B **54** R9678

[20] Timusk T 1999 *Physica* C **317/318** 18
Timusk T and Statt B 1999 *Rep. Prog. Phys.* **62** 61–122

[21] Cardona M 1999 *Physica* C **317/318** 30

[22] Krantz M C, Rosen H J, Macfarlane R M and Lee V Y 1988 *Phys. Rev.* B **38** 4992
Ruf T and Cardona M 1989 *Phys. Rev. Lett.* **63** 2288

[23] Dunne L J and Spiller T P 1992 *J. Phys.: Condens. Matter* **4** 563

[24] Verheijen A A, Van Ruitenbeek J M, de Bruyn Ouboter R and de Jongh L J 1990 *Nature* **345** 418
[25] Liu W, Clinton T W, Smith A W and Lobb C J 1997 *Phys. Rev.* B **55** 11 802
Lang W, Heine G, Kula W and Sobolewski R 1995 *Phys. Rev.* B **51** 9180
Nakao K, Hayashi K, Utagawa T, Enomoto Y and Koshizuka N 1998 *Phys. Rev.* B **57** 8662
Nagaoka T, Matsuda Y, Obara H, Sawa A, Terashima T, Chong I, Takano M and Suzuki M 1998 *Phys. Rev. Lett.* **80** 3594
[26] Withers R L and Wilson J A 1986 *J. Phys. C: Solid State Phys.* **19** 4809–45
[27] Fung K K, McKernan S, Steeds J W and Wilson J A 1981 *J. Phys. C: Solid State Phys.* **14** 5417–32
McKernan S, Steeds J W and Wilson J A 1982 *Phys. Scr.* T **26** 74
[28] Fournier P, Jiang X, Jiang W, Mao S N, Venkatesan T, Lobb C J and Greene R L 1997 *Phys. Rev.* B **56** 14 149
Gollnik F and Naito M 1998 *Phys. Rev.* B **58** 11 734
Serquis A, Prado F and Caneiro A 1999 *Physica* C **313** 271
[29] Podlesnyak A *et al* 1996 *Physica* C **258** 159
[30] Presland M R, Tallon J L, Buckley R G, Liu R S and Flower N E 1991 *Physica* C **176** 95
[31] Blackstead H A and Dow J D 1999 *J. Low Temp. Phys.* **117** 557
Blackstead H A and Dow J D 1997 *Phys. Rev.* B **55** 6605
[32] Wilson J A 1985 *J. Phys. F: Met. Phys.* **15** 591–608
Wilson J A 1990 *J. Phys.: Condens. Matter* **2** 1683–704
[33] Gofron K, Campuzano J C, Abrikosov A A, Lindros M, Bansil A, Ding H, Koelling D and Dabrowski D 1994 *Phys. Rev. Lett.* **73** 3302
Dagotto E, Nazarenko A and Moreo A 1995 *J. Low Temp. Phys.* **99** 409
[34] Khodel V A, Clark J W and Shaginyan V R 1995 *Solid State Commun.* **96** 353
[35] Manako T and Kubo 1994 *Phys. Rev.* B **50** 6402
Rice J P, Giapintzakis J, Ginsberg D M and Mochel J M 1991 *Phys. Rev.* B **44** 10 158
Hammel P C, Statt B W, Martin R L, Chou F C, Johnson D C and Cheong S-W 1998 *Phys. Rev.* B **57** R712
Ino A, Mizokawa T, Fujimori A, Tamasaku K, Eisaki H, Uchida S, Kimura T, Sasagawa T and Kishio K 1997 *Phys. Rev.* B **79** 2101
[36] Loesser A G, Shen Z-X, Schabel M C, Kim C, Zhang M, Kapitulnik and Fournier P 1997 *Phys. Rev.* B **56** 14 185
[37] Basov D N, Liang R, Bonn D A, Hardy W N, Dabrowski B, Quijada M, Tanner D B, Rice J P, Ginsberg D M and Timusk T 1995 *Phys. Rev. Lett.* **74** 598
[38] Koyama Y, Sasagawa T, Togawa Y, Otzschi K, Shimoyama J, Kitazawa K and Kishio K 1999 *J. Low Temp. Phys.* **117** 551
[39] Hussey N E, Cooper J R, Wheatley J M, Fisher I R, Carrington A, Mackenzie A P, Lin C T and Milat O 1996 *Phys. Rev. Lett.* **76** 122
Willemin M, Rossel C, Hofer J, Keller H, Ren Z F and Wang J H 1998 *Phys. Rev.* B **57** 6137
[40] Aubin H, Behnia K, Ribault M, Gagnon R and Taillefer L 1997 *Phys. Rev. Lett.* **78** 2624
Aubin H, Behnia K, Ribault M, Gagnon R and Taillefer L 1997 *Z. Phys.* B **104** 175
Khlopkin M N, Panova G Kh, Chernoplekov N A and Shikov A A 1997 *JETP Lett.* **66** 715
[41] Mesot J *et al* 1999 *Phys. Rev. Lett.* **83** 840
Mesot J *et al* 1999 *J. Low Temp. Phys.* **117** 365
[42] Kouznetsov K A *et al* 1997 *Phys. Rev. Lett.* **79** 3050
Li Q, Tsay Y N, Suenaga M, Klemm R A, Gu G D and Koshizuka N 1999 *Phys. Rev. Lett.* **83** 4160
[43] Johnston D C and Cho J H 1990 *Phys. Rev.* B **42** 8710 (BSCCO)—see also [49]
Miljak M, Zlatic V, Kos I, Thompson J D, Canfield P C and Fisk Z 1993 *Solid State Commun.* **85** 519 (LSCO)
Miljak M, Collin G, Hamzic A and Zlatic V 1989 *Europhys. Lett.* **9** 723 (YBCO)
[44] Fong H F, Bourges P, Sidis Y, Regnault L P, Ivanov A, Gu G D, Koshizuka N and Keimer B 1999 *Nature* **398** 588
[45] Dai P, Yethiraj M, Mook H A, LIndemer T B and Dogan F 1996 *Phys. Rev. Lett.* **77** 5425
Dai P, Mook H A, Hayden S M, Aeppli G, Perring T G, Hunt R D and Dogan F 1999 *Science* **284** 1344
[46] Walstedt R E, Bell R F and Mitzi D B 1991 *Phys. Rev.* B **44** 7760
Takigawa M and Mitzi D B 1994 *Phys. Rev.* B **73** 1287
[47] Suzuki K, Ichimura K, Nomura K and Takekawa S 1999 *Phys. Rev. Lett.* **83** 616
Matsuda A, Sugita S and Watanabe T 1999 *Phys. Rev.* B **60** 1377
[48] Liu H L, Blumberg G, Klein M V, Guptasarma P and Hinks D G 1999 *Phys. Rev. Lett.* **82** 3524
Opel M, Gotzinger M, Hoffmann C, Nemetsch R, Philipp R, Venturini F, Hackl R, Erb A and Walker E 1999 *J. Low Temp. Phys.* **117** 347
[49] Junod A, Wang K-Q, Tsukamoto T, Triscone G, Revaz B, Walker E and Muller J 1994 *Physica* C **222** 209

[50] Monthoux P, Balatsky A V and Pines D 1992 *Phys. Rev.* B **46** 14 803
Pines and Monthoux P 1995 *J. Phys. Chem. Solids* **56** 1651
Takimoto T and Moriya T 1997 *J. Phys. Soc. Japan* **66** 2459
Takimoto T and Moriya T 1998 *J. Phys. Soc. Japan* **67** 3570
Azami M, Matsuura T and Kuroda Y 1997 *J. Phys. Soc. Japan* **66** 2811
Chubukov A V and Morr D K 1997 *Phys. Rep.* **288** 355
Izyumov Yu A 1999 *Sol. Phys.–Usp.* **42** 215
[51] Meregalli V and Savrasov S Y 1998 *Phys. Rev.* B **57** 14 453
[52] Koller D *et al* 1996 *Phys. Rev. Lett.* **77** 4082
Arcon D, Prassides K, Maniero A-L and Brunel L C 2000 *Phys. Rev. Lett.* **84** 562
Wilson J A 1991 *Physica* C **182** 1
[53] Quintanilla J and Gyorffy B L 2000 *Physica* B to appear
[54] Antipov E V, Putilin S N, Kopnin E M, Capponi J, Chaillout E, Loureiro S M, Marezio M and Santoro A 1994 *Physica* C **235–240** 21
[55] Muroi M 1994 *Physica* C **219** 129
[56] Junod A, Erb A and Renner C 1999 *Physica* C **317/318** 333
Torrón C, Díaz A, Pomar A, Veira J A and Vidal F 1994 *Phys. Rev.* B **49** 13 143
Ramallo M V, Pomar A and Vidal F 1996 *Phys. Rev.* B **54** 4341
Corson J, Mallozzi R, Orenstein J, Eckstein J N and Bozovic I 1999 *Nature* **398** 221
[57] Ando Y, Boebinger G S, Passner A, Kimura T and Kishio K 1995 *Phys. Rev. Lett.* **75** 4662 (LSCO)
Ando Y, Boebinger G S, Passner A, Wang N L, Geibel C and Steglich F 1996 *Phys. Rev. Lett.* **77** 2065 (BSCCO)
[58] Renner C, Revaz B, Kadowaki K, Maggio-Aprile I and Fischer Ø 1998 *Phys. Rev. Lett.* **80** 3606
Vaknin D, Zarestky J L and Miller L L 2000 *Physica* C **329** 109
[59] Anderson P W 1997 *The Theory of Superconductivity in High T_c Cuprates (Princeton Series in Physics)* (Princeton, NJ: Princeton University Press)
[60] Choy J-H, Kwon S-J and Park G-S 1998 *Science* **280** 1589
[61] Gamble F R, Osiecki J H, Cais M, Pisaharody R, DiSalvo F J and Geballe T H 1971 *Science* **174** 493
[62] Tranquada J M, Sternlieb B J, Axe J D, Nakamura Y and Uchida S 1995 *Nature* **375** 561 (see figure 4)
[63] Hayden S M, Aeppli G, Mook H, Rytz D, Hundley M F and Fisk Z 1991 *Phys. Rev. Lett.* **66** 821
[64] Blackstead H A and Dow J D 1999 *Int. J. Mod. Phys.* B **13** 3591
Ye J, Sadewasser S, Schilling J S, Zou Z, Matsushita A and Matsumoto T 1999 *Physica* C **328** 111
Abdelrazek M M, Reyes A P, Kuhns P L and Moulton W G 1999 *Int. J. Mod. Phys.* **13** 3615
[65] Nachumi B *et al* 1996 *Phys. Rev. Lett.* **77** 5421 (see addendum to Wilson and Zahrir [1]—E20)
Nakano T, Momono N, Matsuzaki T, Nagata T, Yokoyama M, Oda M and Ido M 1999 *Physica* C **317–8** 575—note too the paper following the above on substitution of Cu by Li in YBCO
[66] Franck J P and Lawrie D 1994 *Physica* C **235–240** 1503
Franck J P and Lawrie D 1996 *J. Low Temp. Phys.* **105** 801
[67] Obertelli S D, Cooper J P and Tallon J L 1992 *Phys. Rev.* B **46** 14 928
[68] Petkov V, Jeong I-K, Chung J S, Thorpe M F, Kycia S and Billinge S J L 1999 *Phys. Rev. Lett.* **83** 4089
[69] DiSalvo F J, Wilson J A, Bagley B G and Waszczak J V 1975 *Phys. Rev.* B **12** 2220
[70] Kleine B, Fazekas P and Müller-Hartmann E 1992 *Z. Phys.* B **86** 405
Kleine B, Fazekas P and Müller-Hartmann E 1992 *Z. Phys.* B **87** 105
Chubakov A, Gagliano E and Balseiro C 1992 *Phys. Rev.* B **45** 7889
[71] Ueda K, Kontani H, Sigrist M and Lee P A 1996 *Phys. Rev. Lett.* **76** 1932
Zhitomirsky M E and Ueda K 1996 *Phys. Rev.* B **54** 9007
[72] Wilson J A 1984 *NATO ASW* B, vol 113, ed P Phariseau and W M Temmerman (New York: Plenum) pp 657–758
[73] Wilson J A 1972 *Adv. Phys.* **21** 143
[74] Hayden S M, Aeppli G, Mook H A, Perring T G, Mason T E, Cheong S-W and Fisk Z 1996 *Phys. Rev. Lett.* **76** 1344
[75] Lake B, Aeppli G, Mason T E, Schröder A, McMorrow D F, Lefmann K, Isshiki M, Nohara M, Takagi H and Hayden S M 1999 *Nature* **400** 43
[76] Ostertun S, Kiltz J, Wolf T and Bock A 1999 *J. Low Temp. Phys.* **117** 425
[77] Rübhausen M, Guptasarma P, Hinks D G and Klein M V 1998 *Phys. Rev.* B **58** 3462
Also note Martin A A, Sanjurjo J A, Hewitt K C, Wang X-Z, Irwin J C and Lee M J G 1997 *Phys. Rev.* B **56** 8426
[78] Osborn R and Goremychkin E A 1991 *Physica* C **244** 311
[79] Bennett M 1999 *PhD Thesis* University of Bristol
[80] Fedorov A V, Valla T, Johnson P D, Li Q, Gu G D and Koshizuka N 1999 *Phys. Rev. Lett.* **82** 2179

[81] Ishida K, Kitaoka K, Asayama K, Kadowaki K and Mochiku T 1994 *J. Phys. Soc. Japan* **63** 1104
[82] Miyakawa N, Guptasarma P, Zasadzinski, Hinks D G and Gray K E 1998 *Phys. Rev. Lett.* **80** 157
Suzuki M, Watanabe T and Matsuda A 1999 *Phys. Rev. Lett.* **82** 5361
Hudson E W, Pan S H, Gupta A K, Ng K-W and Davis J C 1999 *Science* **285** 58
[83] Zhang H, McKenna M J, Hucho C, Sarma B K, Levy M, Kimura T, Kishio K and Kitazawa K 1996 *Physica* B **219/220** 125
[84] Hanaguri T, Fukase T, Tanaka I and Kojima H 1993 *Phys. Rev.* B **48** 9772
[85] Panagopoulos C, Rainford B D, Cooper J R, Lo W, Tallon J L, Loram J W, Wang Y S and Chu C W 1999 *Phys. Rev.* B **60** 14 617
[86] Ido M, Momono N and Oda M 1999 *J. Low Temp. Phys.* **117** 329
[87] Martin R L 1995 *Phys. Rev. Lett.* **75** 744
[88] Gough C E, Colclough M, Forgan E M, Jordan R G, Keene M, Muirhead C M, Rae A I M, Thomas N, Abell J S and Sutton S 1987 *Nature* **326** 2592
[89] Gammel P L, Bishop D J, Dolan G L, Kwo J R, Murray C A, Schneemeyer L F and Waszczak J V 1987 *Phys. Rev. Lett.* **59** 2592
[90] Ren Y, Xu J-H and Ting C S 1995 *Phys. Rev. Lett.* **74** 3680
Ren Y, Xu J-H and Ting C S 1995 *Phys. Rev.* B **52** 7663 (d-wave)
Ren Y, Xu J-H and Ting C S 1996 *Phys. Rev.* B **53** 2249 (d+s)
[91] Dai P, Mook H A, Hayden S M, Aeppli G, Perring T G, Hunt R D and Dogan F 1999 *Science* **284** 1344
Keimer B, Aksay I A, Bossy J, Bourges P, Fong H F, Milius D L, Regnault L P and Vettier C 1998 *J. Phys. Chem Solids* **59** 2135
[92] Dai P, Mook H A and Dogan F 1998 *Phys. Rev. Lett.* **80** 1738
[93] Norman M R, Ding H, Campuzano J C, Takeuchi T, Randeria M, Yokoya T, Takahashi T, Mochiku T and Kadowaki K 1997 *Phys. Rev. Lett.* **79** 3506
[94] Geshkenbein V B, Ioffe L B and Larkin A I 1997 *Phys. Rev.* B **55** 3173
[95] Schafroth S and Rodriguez-Nunez J J 1997 *Z. Phys.* B **102** 493
Schafroth S, Rodriguez-Nunez J J and Beck H 1997 *J. Phys.: Condens. Matter* **9** L111
[96] Letz M and Gooding R J 1998 *J. Phys.: Condens. Matter* **10** 6931
Letz M and Gooding R J 1998 *Physica* B **241/3** 835
[97] Alexandrov A S 1999 *Physica* C **316** 239
Alexandrov A S and Kabanov V V 1999 *Phys. Rev.* B **59** 13 628
[98] Kallio A, Hissa J, Häyrynen T, Bräysy V, Säkkinen T 1998 *Int. J. Mod. Phys.* B **13** 651
[99] Su G and Suzuki M 1999 *Int. J. Mod. Phys.* B **13** 925
[100] Tolmachev V V 2000 *Phys. Lett.* A **266** 400
[101] Ranninger J and Robin J-M 1997 *Phys. Rev.* B **56** 8330
Ranninger J and Romano A 1998 *Phys. Rev. Lett.* **80** 5643
[102] Ren H-C 1998 *Physica* C **303** 115
[103] Engelbrecht J R, Nazarenko A, Randeria M and Dagotto E 1998 *Phys. Rev.* B **57** 13 406
[104] Capezzali M and Beck H 1999 *Physica* C **317/318** 482
[105] Munzar D, Bernhard C and Cardona M 1999 *Physica* C **312** 121
[106] Jankó B, Maly J and Levin K 1997 *Phys. Rev.* B **56** R11 407
Jankó B, Kosztin I and Levin K 1998 *Int. J. Mod. Phys.* B **12** 3009
Maly J, Jankó B and Levin K 1999 *Phys. Rev.* B **59** 1354
Chen Q, Kosztin I, Jankó B and Levin K 1999 *Phys. Rev.* B **59** 7083
[107] Dai X and Su Z-B 1998 *Phys. Rev. Lett.* **81** 2136
[108] Demler E, Kohno H and Zhang Z-C 1998 *Phys. Rev.* B **58** 5719
Demler E and Zhang Z-C 1998 *Nature* **396** 733
[109] Chubukov A V and Morr D K 1998 *Phys. Rev. Lett.* **81** 4716
Abanov A and Chubukov A V 1999 *Phys. Rev. Lett.* B **59** 13 628
[110] Onufrieva F and Pfeuty P 1999 *Phys. Rev. Lett.* **82** 3136
[111] Yoshikawa H and Moriya T 1999 *J. Phys. Soc. Japan* **68** 1340
[112] Gyorffy B L, Szotek Z, Temmerman W M, Andersen O K and Jepsen O 1998 *Phys. Rev.* B **58** 1025